variables examined included demographic data, cardiac diagnosis, date of surgery, details of operative procedure, echocardiographic data, catheterization data, laboratory data, the length of postoperative hospital stay, duration of mechanical ventilation, duration of chest tube drainage, and outcomes. The inclusion criteria for "one lung" in this study is 100% occlusion of either the right or left pulmonary artery (PA).

Data Analysis

Data are expressed as the mean (SD) or median and range, as appropriate. To determine the risk factors for mortality, univariate and multivariate analyses were performed. Binary data and continuous data were analyzed using Fisher's exact test and the unpaired *t* test, respectively. Calculation of survival was performed by the Kaplan-Meier method. Cox proportional hazard analysis was used for multivariate analysis. A *p* value less than 0.05 was considered statistically significant.

Results

Patient Characteristics and Pre-Fontan Data

The detailed characteristics of each patient are provided in Table 1. The median age at the time of one-lung Fontan operation was 3.5 years (range, 1.0 to 22.8). The median height was 89 cm (range, 66 to 171) and the median body weight was 11.0 kg (range, 6.3 to 45.4). All these patients had previously undergone numerous cardiac operations, with a median of 4 (range, 2 to 5) per patient. Eleven of the 12 patients (92%) had undergone a bidirectional Glenn operation previously. The available lung was right in 9 patients (75%) and left in 3 patients (25%). Potential causes of unilateral obstruction of the PA were pulmonary venous obstruction (PVO) in 8 patients and PA thromboembolism in 4 patients. These pulmonary obstructions were caused before Fontan operation in 11 patients and early after Fontan operation in 1 patient.

Blood examination revealed the hemoglobin concentration, hematocrit, and platelet count were 16.9 ± 2.8 g/dL (range, 12.4 to 22.5), 51.7% ± 2.8% (range, 39.7 to 63.1), and 272 ± 74 × $10^3/\mu L$ (158 to 366), respectively. The total protein and albumin was 7.4 ± 0.7 mg/dL (range, 6.2 to 9.0) and 4.5 ± 0.5 mg/dL (range, 3.8 to 5.1), respectively. The aspartate transaminase and alanine transaminase concentrations were 36 ± 20 IU/L (range, 17 to 91) and 21 ± 14 U/L (range, 8 to 90), respectively. The total bilirubin concentration was 0.7 ± 0.4 mg/dL (range, 0.3 to 1.5). The creatinine concentration was 0.49 ± 0.28 mg/dL (range, 0.28 to 1.10). The arterial oxygen saturation was 83% ± 7% (range, 69 to 92). The mean available pulmonary arterial pressure (mPAP), atrial pressure, and ventricular end-diastolic pressure were 11.5 ± 3.3 mm Hg (range, 7.0 to 18.0), 5.9 ± 2.9 mm Hg (range, 2.0 to 12.0), and 7.5 ± 3.5 mm Hg (range, 1.0 to 12.0), respectively. The ventricular ejection fraction was 58% ± 13% (range, 39 to 76). The grade of atrioventricular valve regurgitation (AVVR) was none in 3 patients, trivial in 6 patients, and mild in 2 patients. The grade of AVVR was not recorded clearly in 1 patient: however, it was mild or lower.

Surgical Data

The technique used for the one-lung Fontan operation was extracardiac TCPC in 10 patients, intraatrial extracardiac TCPC in 1 patient, and an atriopulmonary connection in 1 patient. Associated procedures included creation of a fenestration in 7 patients, pulmonary arterial plasty in 2 patients, release of the PVO in 1 patient, and plication of the left diaphragm in 1 patient. The cardiopulmonary bypass time was 151 ± 64 minutes (range, 60 to 243). An aortic cross-clamp was performed in 7 patients, with duration of 46 ± 25 minutes (range, 11 to 84). Modified ultrafiltration was used in 10 patients.

Early Outcomes

No patient died within 30 days after the operation. There was 1 in-hospital death (patient no. 5 in Table 1). This patient had a cerebral infarction at an extracardiac TCPC, complicated by severe right-side pneumonia, and she died 85 days after the operation. For the hospital survivors, the median duration of mechanical ventilator support was 14 hours (range, 0 to 768). The median duration of the requirement for chest drainage was 8 days (range, 5 to 78). One patient required bilateral chemical pleural adhesion therapy owing to persistent pleural effusion (patient no. 11 in Table 1). This patient could be weaned off chest drainage on postoperative day 78 and required home oxygenation therapy after discharge. The median postoperative hospital stay was 72 days (interquartile range, 40 to 122). The median maximum postoperative serum creatinine concentration was 0.71 mg/dL (range, 0.41 to 6.70). The grade of AVVR at the time of discharge was none in 3 patients, trivial in 6 patients, and mild in 2 patients. The other major early postoperative complications were pneumonia of unavailable lung in 2 patients, mediastinitis with left pyothorax (the available lung is right) in 1 patient, renal dysfunction requiring dialysis in 2 patients, bradycardia with junctional rhythm in 1 patient, and paroxysmal supraventricular tachyarrhythmia in 1 patient.

Midterm to Long-Term Outcomes

There were 2 late deaths among the 11 hospital survivors with the mean follow-up period of 8.1 ± 6.5 years (range, 0.5 to 21.3). One patient was a 2-year-old boy (patient no. 6 in Table 1) who underwent an extracardiac TCPC. He had pneumonia 2 years after the operation and died. The other patient was a 21-year-old man (patient no. 11 in Table 1) who underwent an extracardiac TCPC and required pleural adhesion therapy as described above. He had protein-losing enteropathy 2 years after the operation and was managed with steroid, albumin, and gamma-globulin. But his course was complicated by severe fungal pneumonia, and he died 3 years after the operation. The estimated overall survival was 83%, 73%, and 73% at 1, 5, 10 years after the operation, respectively (Fig 1).

Regarding the present level of activity of the 4 adult survivors, 1 patient is working as an officer, 1 is a

Table 1. Patient Characteristics and Final Outcomes

Pt. No.	Age, Years	Sex	HT, cm	BW, kg	Main Diagnosis	Previous Operations (Age at Operation)	Available Lung	Cause of One Lung	Final Outcome
1	14.4	M	159	43	PAIVS	Lt mBTS (1 mon) BDG+ASD creation (3 y), re-Lt mBTS (8 y) IPAS+CS+PAP+Lt PVO release (13 y)	Right	Lt PVO	Alive
2	3.3	M	88	11	MA, DORV, CoA	CoA repair (EEA)+PAB (2 mon) DKS+mBTS (2 mon), BDG (8 mon) Lt PVO release+TVP+CS+IPAS (2 y) Lt PVO release (3 y)	Right	Lt PVO	Alive
3	22.8	F	151	43	CAVC, DORV, PS, asplenia	Lt mBTS (14 mon), CS (4 y), Lt BDG	Left	Rt PAO	Alive
4	1.0	F	66	6	SLV, CAVC, PA	Rt mBTS (2 mon), Lt mBTS (3 mon) Lt PVO release+PAP (5 mon) BDG+Lt mBTS+PAP (7 mon)	Right	Lt PVO	Alive
5	2.0	F	86	11	SA, SRV, PA, TGA, TAPVC(2b), asplenia	PVO release+RVPAS (2 mon) IPAS+BDG+Rt shunt with ITA (13 mon) Rt PVO release (17 mon)	Left	Rt PVO	Dead
6	2.2	M	80	9	HLHS	Norwood (RVPAS) (7 days) BDG+ASD creation+RV aneurysmectomy (6 mon) IPAS+Lt mBTS+PAP+Lt PVO release (15 mon) Lt PVO release (22 mon)	Right	Lt PVO	Dead
7	3.7	M	84	9	CAVC, DORV, SA, TAPVC(1b)	TAPVC repair+PAB (8 days) BDG+IPAS+re-PAB, PVO release+CAVVP (6 mon) CS(4)+CAVVP (16 mon) Lt PVO release+CAVVP (2 y)	Right	Lt PVO	Alive
8	5.4	M	108	16	TA(Ib)	Rt oBTS (12 mon), Lt mBTS (20 mon)	Left	Rt PA stenosis	Alive
9	2.2	M	70	7	DORV, SAS, CoA	CoA repair+PAB (11 days), Re-CoA repair+ASD creation (2 mon), VSD enlargement+PAP+RVPAS (7 mon) BDG+DKS (14 mon)	Right	Lt PVO	Alive
10	17.9	F	150	35	TA(IIA), PA	Lt mBTS(2 y), CS (9 y), CS (13 y) BDG (18 y)	Right	Lt lower PVO Lt PAO	Alive
11	21.3	M	171	45	SRV	Lt mBTS (2 mon), BDG (3 y)	Right	Lt PAO	Dead
12	2.2	M	89	10	SLV	PAB (2 mon) BDG+DKS+CAVVP+PAP (12 mon)	Right	Paralysis of Lt diaphragm	Alive

ASD = atrial septal defect; BDG = bidirectional Glenn operation; BW = body weight; CAVC = common atrioventricular septal defect; CAVVP = common atrioventricular valve plasty; CoA = coarctation of aorta; CS = central shunt; DKS = Damus-Kaye-Stansel anastomosis; DORV = double outlet right ventricle; EEA = end-to-end anastomosis; F = female; HLHS = hypoplastic left heart syndrome; HT = height; IPAS = intrapulmonary artery septation; ITA = internal thoracic artery; Lt = left; M = male; MA = mitral atresia; mBTS = modified Blalock-Taussig shunt; mon = months; oBTS = original Blalock-Taussig shunt; PA = pulmonary atresia; PAB = pulmonary arterial banding; PAIVS = pulmonary atresia with intact ventricular septum; PAO = pulmonary arterial obstruction; PAP = pulmonary arterial plasty; PS = pulmonary stenosis; PVO = pulmonary venous obstruction; Rt = right; RV = right ventricle; RVPAS = right ventricle–pulmonary artery shunt; SA = single atrium; SAS = subaortic stenosis; SLV = single left ventricle; SRV = single right ventricle; TA = tricuspid atresia; TAPVC = total anomalous pulmonary venous connection; TGA = transposition of the great arteries; TVP = tricuspid valve plasty; VSD = ventricular septal defect; y = years.

university student, and 2 other patients are at home under treatment without working or attending school. Five patients are still of the pediatric age and are under treatment in an outpatient clinic. The New York Heart Association functional class was grade 1 in 4 patients, grade 2 in 3 patients, grade 3 in 2 patients, and unknown in 1 patient (the latter patient is being followed up by a local outpatient clinic now, but there is no exact information about New York Heart Association class on the questionnaire).

Surgical intervention was required in 1 patient. The patient underwent ligation or division of well-developed arteriopulmonary collateral arteries (patient no. 7 in Table 1). In addition, 2 patients underwent a catheter-based intervention: 1 who had undergone an atriopulmonary connection was treated with percutaneous release of a stenosis of atriopulmonary connection (patient no. 8 in Table 1); the other required coil embolization of the bronchial, intercostal, and inferior diaphragmatic arteries for the treatment of hemoptysis (patient no. 12 in Table 1). One patient required home oxygenation therapy (patient no. 9 in Table 1). One patient had paroxysmal atrial fibrillation (patient no. 8 in Table 1). One patient had repeated bronchitis (patient no. 2 in Table 1).

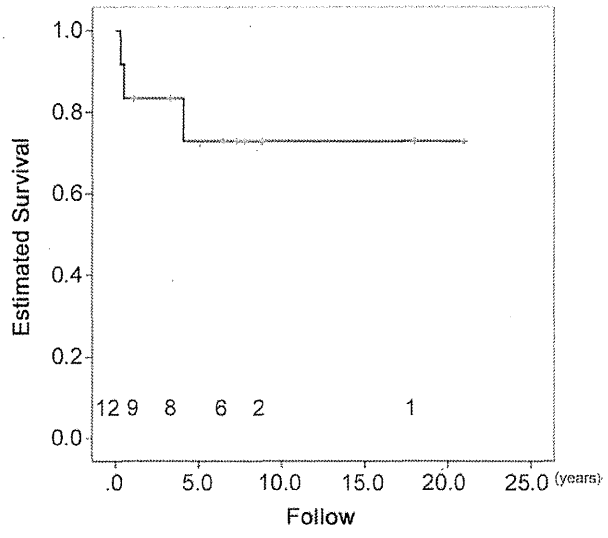

Fig 1. Estimated actuarial survival in patients who underwent one-lung Fontan operation. Actuarial survival was 83% at 1 year, 73% at 5 years, and 73% at 10 years after operation.

On blood examination in the late survivors, the hemoglobin concentration, hematocrit, and platelet count were 14.7 ± 3.3 g/dL (range, 10.5 to 18.9), 43.8% ± 8.7% (range, 31.5 to 54.2), and 165 ± 120 × $10^3/\mu L$ (range, 143 to 356), respectively. The total protein and albumin was 7.1 ± 0.5 mg/dL (range, 6.2 to 8.0) and 4.2 ± 0.8 mg/dL (range, 2.7 to 5.1), respectively. The aspartate transaminase and alanine transaminase concentrations were 27 ± 8 IU/L (range, 21 to 43) and 14 ± 6 U/L (range, 7 to 21), respectively. The total bilirubin concentration was 0.7 ± 0.4 mg/dL (range, 0.3 to 1.4). The creatinine concentration was 0.52 ± 0.32 mg/dL (range, 0.18 to 1.00).

Postoperative cardiac catheterization was performed in 7 patients. The arterial oxygen saturation was 90% ± 9% (range, 71 to 97). The average mPAP, ventricular end-diastolic pressure, and ventricular ejection fraction were 11.1 ± 0.9 mm Hg (range, 10.0 to 12.0), 9.5 ± 3.3 mm Hg (range, 6.0 to 14.0), and 63% ± 12% (range, 48 to 86), respectively.

The grade of the AVVR in the late survivors was mild or lower in 8 patients, and moderate in 1 patient.

Risk Analysis of Overall Mortality

By univariate analysis, impaired ventricular function was a significant risk factor for mortality (43.0% ± 9.5% in dead cases versus 64.0% ± 9.5% in living cases, $p < 0.01$). There was no significant association with differences in the availability of the right lung, sex, presence of a fenestration, use of aortic cross-clamp, use of modified ultrafiltration, age, body weight, hemoglobin, hematocrit, platelet count, total protein, albumin, aspartate transaminase, alanine transaminase, serum total bilirubin, arterial oxygen saturation, mPAP, ventricular end-diastolic pressure, cardiopulmonary bypass time, aortic cross-clamp time, duration of chest drainage, duration of the hospital stay, and maximum creatinine level after operation. By multivariate analysis, there was no significant risk factor for mortality.

Comment

Sade and associates [9] first described a one-lung Fontan operation. They reported a 10-year-old patient who successfully underwent right-side one-lung Fontan operation using a Dacron conduit between the right atrium and the right PA [9] and clinically doing well 9 years after the operation [10]. In addition, Zachary and colleagues [11] reported 7 cases of one-lung Fontan operation in 1998. They investigated the postoperative differences between patients with one lung and two lungs and reported that only difference between these two groups was noted in the postoperative arterial oxygen saturation (87% in the one-lung group versus 91% in the two-lungs group) [11]. Then, their group described the results of 5 long-term survivors of these 7 cases and their additional 5 cases of one-lung Fontan operation in 2004 [12]. The total number of reported one-lung Fontan operations including this study was 28 [9–15]. There was 1 hospital death (3.6%) and 5 late deaths (17.9%). Three of the 6 deaths were from this report. The other 3 late deaths were reported by the group of Zachary and coworkers [11, 14]. The overall mortality was 21.4%. The mortality in this report seems to be worse than overall mortality of the Fontan operation reported from Japan [16, 17]. However, it is notable that the mortality was 0% in one-lung Fontan patients with ventricular ejection fraction more than 50% with a follow-up period of 9.2 ± 6.9 years (range, 1.1 to 21.0). Considering the recent survival of pediatric heart transplantation is less than 70% at 10 years and less than 50% at 20 years [18], one-lung Fontan operation could be better option in selected patients. Conversely, patients with either impaired ventricular or pulmonary condition might be contraindicated for one-lung Fontan operation.

One case of PLE was diagnosed in this study. All of the other late survivors had no symptoms indicating PLE. However, 1 patient had serum albumin concentration of 2.7 mg/dL. This finding is very suspect for PLE; unfortunately, however, there is no information about stool alpha-1-antitrypsin level. No other patients had serum albumin concentration of less than 3.5 mg/dL. The incidence of the PLE in this study was 8.3% (16.7% if including 1 suspected case); however, Jacobs and colleagues [11] reported that 50% of the one-lung Fontan patients had PLE. To know the reason why this difference occurred is difficult. However, judging from the data of their first 7 cases (mean pulmonary arterial pressure 11.7 ± 2.7 mm Hg, mean atrial pressure 6.0 ± 3.6 mm Hg, and mean ventricular end-diastolic pressure 7.9 ± 2.7 mm Hg) [11] and the data of their additional 5 cases that they described [12], the preoperative pulmonary and cardiac condition for one-lung Fontan operation seems to be comparable between their report and this report. The follow-up period of their cases seems not to be extremely different from that of this report, although we could not know the exact follow-up period of their report. Concerning the method of Fontan procedure, 11 of 12 patients underwent a lateral tunnel

type of TCPC with or without partial hepatic vein exclusion or fenestration in their study. In this study, 11 of 12 patients underwent extracardiac or intraatrial extracardiac conduit TCPC with or without fenestration. Although the selection of the procedures may affect the incidence of the PLE, there has been no way to elucidate it. Further investigation should be required to determine the optimal surgical method for one-lung Fontan operation.

Pulmonary condition of the available lung is obviously crucial for one-lung Fontan operation. In this report, all patients except for 1 who underwent one-staged Fontan completion had mPAP of 15 mm Hg or less. Although mPAP in this patient was 18 mm Hg, the pulmonary arterial resistance was 1.4 Woods unit · m^2. We could not reach any conclusion about the borderline of pulmonary arterial resistance for one-lung Fontan operation in this study.

In this study, there is no true unilateral pulmonary atresia or hypoplasia. All unilateral pulmonary obstructions were caused by thromboembolism secondary to PVO or severe PA stenosis. Although one-lung Fontan operation seems to be a viable option, efforts to reconstruct the occluded PA should be challenged in such cases. Increasing available pulmonary vascular bed would be beneficial for the patient. Schmauss and coworkers [19] reported a case of successful reconstruction of an occluded right PA due to thromboembolism. The right PA was reconstructed with catheter intervention in this patient before the Fontan operation and was patent 3 years after the operation [19]. Tchervenkov and associates [20] described a successful case of intrapulmonary reconstruction of the left PA. Jacobs and associates [12] also said that PA reconstruction with homograft vascular patch could be successful in a few patients. They also said Blalock pulmonary shunt and PA reconstruction using cryopreserved saphenous vein and transcatheter stent could be a possible option for the PA reconstruction [12]. Reconstruction of PVO should also be tried using the same reasoning [19]; however, the recurrence rate will be high in such cases.

Cardiac function is an important factor for deciding the indication for Fontan operation [21, 22]. Although recent improvement of management strategy for Fontan operation have improved clinical outcomes [23], ventricular dysfunction and AVVR should affect the early or late outcomes, especially in patients with impaired pulmonary function. In this report, both of 2 patients with late deaths after the discharge had low systemic ejection fractions, 39% and 40%, respectively. One of them had postoperative PLE. The causes of both deaths were pneumonia; however, low output state in the background may have affected their outcome. Lower preoperative ventricular ejection fraction was a significant risk factor in univariate analysis, but not in multivariate analysis in this study. Although we could not reach any conclusion about this issue, normal ventricular function is believed to be desirable for successful one-lung Fontan operation. Regarding AVVR, all of the patients had competent atrioventricular valve function before Fontan operation in this report. One patient had moderate AVVR postoperatively probably due to increased arteriopulmonary collateral flow after one-lung Fontan operation. However, this patient did clinically well with serum B-type natriuretic peptide level of 44 pg/mL after coil embolizations of arteriopulmonary collateral arteries.

A major limitation of this study is the small number of patients. Further accumulation of data of one-lung Fontan circulation should be required to reach true conclusions to determine the boundary of one-lung Fontan operations.

In conclusion, absence of one lung itself is not a contraindication for the Fontan operation. No mortality from one-lung Fontan operation was observed among patients with both good available lung and ventricular functions. However, moderately and severely impaired ventricular function may be contraindications for one-lung Fontan operation.

References

1. Fontan F, Baudet E. Surgical repair of tricuspid atresia. Thorax 1971;26:240–8.
2. de Leval MR, Kilner P, Gewillig M, Bull C. Total cavopulmonary connection: a logical alternative to atriopulmonary connection for complex Fontan operations. Experimental studies and early clinical experience. J Thorac Cardiovasc Surg 1988;96:682–95.
3. Giannico S, Corno A, Marino B, et al. Total extracardiac right heart bypass. Circulation 1992;86(Suppl 2):110–7.
4. Balaji S, Gewillig M, Bull C, de Leval MR, Deanfield JE. Arrhythmia after Fontan procedure: comparison of total cavopulmonary connection and atriopulmonary connection. Circulation 1991;84(Suppl):III162–7.
5. Gentles TL, Mayer JE, Gauvreau K, et al. Fontan operation in five hundred consecutive children: factors influencing early and late outcome. J Thorac Cardiovasc Surg 1997;114:376–91.
6. Masuda M, Kado H, Shiokawa Y, et al. Clinical results of the staged Fontan procedure in high-risk patients. Ann Thorac Surg 1998;65:1721–5.
7. Bridges ND, Mayer JE, Lock JE, et al. Effect of baffle fenestration on outcome of the modified Fontan operation. Circulation 1992;86:1762–9.
8. Gaynor JW. The effect of modified ultrafiltration on the postoperative course in patients with congenital heart disease. Semin Thorac Cardiovasc Surg Pediatr Card Surg Annu 2003;6:128–39.
9. Sade RM, Riopel DA, Taylor AB. Orthoterminally corrective operation in the presence of severe hypoplasia of a pulmonary artery. J Thorac Cardiovasc Surg 1980;80:424–6.
10. Sade RM, Gillette PC. Fontan operation in a case of single functional pulmonary artery. J Thorac Cardiovasc Surg 1989; 98:153–4.
11. Zachary CH, Jacobs ML, Apostolopoulou S, Fogel MA. One-lung Fontan operation: hemodynamics and surgical outcome. Ann Thorac Surg 1998;65:171–5.
12. Jacobs ML, Schneider DJ, Pourmoghadam KK, Pizarro C, Norwood WI. Total cavopulmonary connection to one lung. Ped Card Surg Ann Semin Thorac Cardiovasc Surg 2004;7: 72–9.
13. Pereira A, Ferreira R, Anjos R, et al. Hemoptysis in a single lung Fontan: percutaneous approach. Rev Port Cardiol 2009; 28:1399–403.
14. Al-Khaldi A, Chedrawy EG, Tchervenkov CI, Shum-Tim D. Ann Thorac Surg 2005;79:1042–4.
15. Subbareddy K, Chaudhuri S, Neligan M. Unilateral Fontan operation for tricuspid atresia. Case report. Scand J Thorac Cardiovasc Surg 1996;30:97–9.

16. Ohuchi H, Kagisaki K, Miyazaki A, et al. Impact of the evolution of the Fontan operation on early and late mortality: a single-center experience of 405 patients over 3 decades. Ann Thorac Surg 2011;92:1457–67.
17. Nakano T, Kado H, Tachibana T, Hinokiyama K, et al. Excellent midterm outcome of extracardiac conduit total cavopulmonary connection: results of 126 cases. Ann Thorac Surg 2007;84:1619–26.
18. Kirk R, Edwards LB, Kucheryavaya AY, et al. The registry of the International Society for Heart and Lung Transplantation: fourth pediatric heart and lung transplantation report—2011. J Heart Lung Transplant 2011;30:1071–132.
19. Schmauss D, Kaczmarek I, Sachweh J, et al. Successful single lung Fontan operation in 2 children: case reports. Heart Surg Forum 2007;10:E331–3.
20. Tchervenkov CI, Chedrawy EG, Korkola SJ. Fontan operation for patients with severe distal pulmonary artery stenosis, atresia, or a single lung. Semin Thorac Cardiovasc Surg Pediatr Card Surg Annu 2002;5:68–75.
21. Hosein RBM, Clarke AJB, McGuirk SP, et al. Factors influencing early and late outcome following the Fontan procedure in the current era. The "Two Commandments"? Eur J Cardiothorac Surg 2007;31:344–53.
22. Yoshimura N, Yamaguchi M, Oshima Y, et al. Risk factors influencing early and late mortality after total cavopulmonary connection. Eur J Cardiothorac Surg 2001;20:598–602.
23. Kotani Y, Kasahara S, Fujii Y, et al. Clinical outcome of the Fontan operation in patients with impaired ventricular function. Eur J Cardiothorac Surg 2009;36:683–7.

DISCUSSION

DR YVES D'UDEKEM D'ACOZ (Victoria, Australia): There is a saying that you should not do a bad Fontan, you should do only a good Fontan. And I think that I am still of the same opinion after having heard your excellent presentation. I think we needed the numbers you presented, it was very interesting. But when I look at your numbers, 25% of your patients died within 5 years and another 25% suffer from failure because you have 1 patient suffering from protein-losing enteropathy and 2 patients in NYHA class III. And I think we all know what it means to be a failing Fontan: these patients are very limited. So if you have 50% chance of success, what do you think that we should offer to the patient having seen these results? Should we offer heart transplantation or should we offer Fontan on one lung?

DR FUJII: I think I can understand your concern, but there is a very specific situation in Japan. Heart transplantation for children has been inhibited for a long time. Recently, heart transplantation for children became legal, but we still cannot find any heart transplantation donor for young children because of the social situation in Japan. I think it is spiritual or religious kind of thing. So we had no other choice. This is why these patients underwent one-lung Fontan operation.

Actually, the mortality is higher than the two-lung Fontan operation. The mortality is 25%. But some patients can spend an almost normal social life. The last patient I presented had survived for 19 years and can work as an office worker without any symptoms. So we have to think about the one-lung Fontan operation, I think.

DR SANO: I will answer your questions. Most of these patients are of the period where we are not allowed to do transplant, but it is clear that these one-lung patients who had the impaired ventricular function are very worse. So these patients may be a candidate of transplant. But the patient who had the reasonably good ventricular function, even these patients had one-lung Fontan, the long-term result is not bad. And I think that even transplant after the failed Fontan is not a very good long-term result.

Atherosclerosis 220 (2012) 134–138

Contents lists available at SciVerse ScienceDirect

Atherosclerosis

journal homepage: www.elsevier.com/locate/atherosclerosis

Four-year clinical outcomes of the OLIVUS-Ex (impact of Olmesartan on progression of coronary atherosclerosis: Evaluation by intravascular ultrasound) extension trial

Atsushi Hirohata[a,*], Keizo Yamamoto[a], Toru Miyoshi[e], Kunihiko Hatanaka[b], Satoshi Hirohata[b], Hitoshi Yamawaki[c], Issei Komatsubara[d], Eiki Hirose[a], Yuhei Kobayashi[a], Keisuke Ohkawa[a], Minako Ohara[a], Hiroya Takafuji[a], Fumihiko Sano[a], Yuko Toyama[a], Shozo Kusachi[b], Tohru Ohe[a], Hiroshi Ito[e]

[a] *The Sakakibara Heart Institute of Okayama, Japan*
[b] *Okayama University Graduate School of Medicine, Dentistry and Pharmaceutical Sciences, Okayama, Japan*
[c] *Tottori City Hospital, Tottori, Japan*
[d] *Tsuyama Central Hospital, Tsuyama, Japan*
[e] *Okayama University, Department of Cardiovascular Medicine, Okayama, Japan*

ARTICLE INFO

Article history:
Received 15 July 2011
Accepted 4 October 2011
Available online 9 November 2011

Keywords:
Arteriosclerosis
Atherosclerosis
Ultrasonics
Prevention
Angiotensin

ABSTRACT

Background: The previous OLIVUS trial reported a positive role in achieving a lower rate of coronary atheroma progression through the administration of Olmesartan, an angiotension-II receptor blocking agent (ARB), for stable angina pectoris (SAP) patients requiring percutaneous coronary intervention (PCI). However, the benefits between ARB administration on long-term clinical outcomes and serial atheroma changes by IVUS remain unclear. Thus, we examined the 4-year clinical outcomes from OLIVUS according to treatment strategy with Olmesartan.
Methods: Serial volumetric IVUS examinations (baseline and 14 months) were performed in 247 patients with hypertension and SAP. When these patients underwent PCI for culprit lesions, IVUS was performed in their non-culprit vessels. Patients were randomly assigned to receive 20–40 mg of Olmesartan or control, and treated with a combination of β-blockers, calcium channel blockers, glycemic control agents and/or statins per physician's guidance. Four-year clinical outcomes and annual progression rate of atherosclerosis, assessed by serial IVUS, were compared with major adverse cardio- and cerebrovascular events (MACCE).
Results: Cumulative event-free survival was significantly higher in the Olmesartan group than in the control group ($p = 0.04$; log-rank test). By adjusting for validated prognosticators, Olmesartan administration was identified as a good predictor of MACCE ($p = 0.041$). On the other hand, patients with adverse events ($n = 31$) had larger annual atheroma progression than the rest of the population (23.8% vs. 2.1%, $p < 0.001$).
Conclusions: Olmesartan therapy appears to confer improved long-term clinical outcomes. Atheroma volume changes, assessed by IVUS, seem to be a reliable surrogate for future major adverse cardio- and cerebrovascular events in this study cohort.

1. Background

Despite the widespread application of established medical therapies, extensive cardiovascular disease remains the most important cause of morbidity and mortality in patients with ischemic coronary disease [1–11]. Although angina pectoris is characterized by a clustering of cardiovascular disease risk factors, such as dyslipidemia, diabetes, and hypertension, optimal atheroma management is a key strategy for preventing subsequent cardiovascular events [1,4–10,12–16]. Prior intravascular ultrasound (IVUS) trials reported a slowing of coronary atheroma progression or regression with some medicines, however, the direct benefits between drug administration on long-term clinical outcomes and atheroma volume changes, assessed by IVUS, have not been well clarified [1,4–10,12–16].

The OLIVUS trial, using serial volumetric IVUS, reported a positive role in achieving a lower rate of coronary atheroma progression through the administration of Olmesartan, an angiotension-II

* Corresponding author at: Cardiovascular Medicine, The Sakakibara Heart Institute of Okayama, 2-1-10, Marunouchi, Okayama 700-0823, Japan.
Tel.: +81 86 225 7111; fax: +81 86 223 5265.
E-mail address: hirohata@tg7.so-net.ne.jp (A. Hirohata).

0021-9150/$ – see front matter © 2011 Elsevier Ireland Ltd. All rights reserved.
doi:10.1016/j.atherosclerosis.2011.10.013

receptor blocking agent (ARB), for stable angina pectoris (SAP) patients requiring percutaneous coronary intervention (PCI) [17]. According to treatment strategy with Olmesartan, we investigated the 4-year OLIVUS follow up data to evaluate the relation between atheroma volume change and clinical outcomes.

2. Methods

2.1. Patients and study design

The OLIVUS trial is a prospective, randomized, multicenter trial which examined the impact of Olmesartan on the progression of coronary atherosclerosis; evaluation by intravascular ultrasound (OLIVUS) [17]. Patients with hypertension and clinically stable angina pectoris scheduled for percutaneous coronary intervention (PCI) were enrolled. After PCI for their culprit lesions, IVUS was performed over 40 mm in their non-culprit vessels, defined as without angiographically documented coronary stenosis <50%, to determine plaque volume at baseline. Hemodynamically unstable patients, recent myocardial infarction within 4 weeks, ejection fraction <25%, and patients already on ACE inhibitors or ARBs were excluded from the trial. Patients were randomized to control or Olmesartan 10–40 mg titrated to maximally tolerated dose by 8 weeks. In addition, patients were treated with a combination of β-blockers, calcium channel blockers, diuretics, nitrates, glycemic control agents and/or statins per physician's guidance. After 12–16 months, IVUS of the originally examined coronary artery was performed during the routine follow-up angiogram. The extended-OLIVUS trial increased the follow-up period of the OLIVUS trial to evaluate associations between clinical prognosis, coronary atheroma changes and Olmesartan treatment. The study protocol was approved by all participating institutional review boards and all patients provided written informed consent. The primary endpoint was the incidence of major adverse cardio- and cerebrovascular events (MACCE), including the composite of death from cardiac or cerebral causes, myocardial infarction, stroke, rehospitalization due to unstable or progressive angina according to the Braunwald unstable angina classification and the Canadian Cardiovascular Society angina classification, deterioration of heart function or renal failure. Stroke was diagnosed based on the presence of a neurologic deficit confirmed by computed tomography or magnetic resonance imaging. Outcome data were collected by serial contact with the patients or their families until July 31, 2011. Medical records of patients who died or who were treated at participating hospitals were analyzed.

2.2. Intravascular ultrasound

IVUS studies were performed using a commercially available imaging system with a 40-MHz mechanical transducer ultrasound catheter (Boston Scientific Corporation, Natick, MA). Using automated pullback (0.5 mm/s), ultrasound images were obtained and recorded for off-line quantitative analysis. The images were digitized and three-dimensional volumetric analysis was performed using Simpson's method (EchoPlaque, Indec Systems, Mountain View, CA). Measurements included vessel, lumen and atheroma volumes (ATV) over the 40 mm segment in the non-PCI-culprit vessels. To standardize for vessel size, percent atheroma volume (%ATV), defined as plaque volume divided by vessel volume, was also calculated. The serial progression rate of atherosclerosis was compared with change in absolute atheroma volume and change in percent atheroma volume, measured by (follow-up ATV − baseline ATV)/baseline ATV, and (follow-up %ATV − baseline %ATV)/baseline %ATV, respectively. All analytic methods were previously reported [17,18].

Table 1
Baseline patient characteristics and medications.

	Control ($n=121$)	Olmesartan ($n=126$)	p
Gender (male, %)	68	76	ns
Age (years)	68.4 ± 8.8	67.8 ± 8.7	ns
Smoking (%)	31	34	ns
Diabetes (%)	35	31	ns
Previous MI (%)	13	15	ns
Aspirin (%)	100	100	ns
β-Blocker (%)	13.2	12.7	ns
Calcium channel blockers (%)	49.6	41.3	ns
Statins (%)	74.0	71.4	ns
Oral diabetic agents (%)	17.3	19.8	ns
Insulin (%)	7.1	5.6	ns

2.3. Statistical methods

Analyses were performed using SPSS 11 software (SPSS Inc., Chicago, IL). Laboratory and ultrasound parameters were reported as the mean value ± SD. Continuous variables are expressed as means ± SD. Data from two independent groups were compared using a t-test or Wilcoxon rank-sum test. Intra-group data were analyzed using a paired t-test or the Wilcoxon signed-rank test. Categorical data were tabulated as frequencies and percentages and compared using the χ^2 test or Fisher's exact test. Event-free survival probabilities for MACCE were estimated using the Kaplan–Meier method and group differences were assessed using a log-rank test. Unadjusted hazard ratios for variables, namely administration of Olmesartan, statin, age, gender, atheroma volume changes, baseline percent atheroma volume, hypertension, diabetes, smoking, prior history of coronary artery disease and baseline LDL-C values, were calculated using the Cox proportional hazards model. A two-sided p-value of <0.05 was considered significant.

3. Results

Between February 2006 and August 2007, 247 patients with stable angina pectoris patients undergoing PCI were enrolled in this trial. Prognostic data were fully documented during the entire follow-up period (mean duration, 4.1 ± 1.3 years). During follow up, 15 patients in the control group and 17 patients in the Olmesartan group dropped out of the trial because of MACCE, laboratory abnormality or having withdrawn consent. Even though serial volumetric IVUS analyses were completed in 205 patients, vital status was ascertained in 233 (93.3%) patients at the end of the study. Of the 118 (93.6%) patients taking Olmesartan at the end of the study, 107 (84.9%) were on the full dose (20–40 mg), with only 4 (3.2%) on a reduced dose.

3.1. Patient characteristics and blood pressure changes

Patient characteristics and medications are summarized in Tables 1 and 2. All data are identical between the control and Olmesartan groups. Serial changes in blood pressure are presented in Fig. 1. In this trial, blood pressure control was at the physician's discretion except for administration of Olmesartan. While significant improvement in blood pressure, LDL/HDL cholesterol and glycemic control were observed in both groups, there was no significant difference between the control and Olmesartan group.

3.2. Volumetric IVUS analysis

Significant development of atheroma volume (ATV) and percent atheroma volume (%ATV) was found in the control group between baseline and 14-months follow-up (from 208.8 ± 151.5 to 215.9 ± 156.8 (mm^3), $p<0.01$ for ATV, from 40.6 ± 10.8 to

Table 2
Blood parameters of patients at baseline and 4-years follow-up.

	Baseline			Follow-up		
	Control	Olmesartan	p-Value	Control	Olmesartan	p-Value
Total cholesterol (mg/dl)	185.9 ± 34.3	183.3 ± 29.6	0.554	183.8 ± 37.0	181.4 ± 30.4	0.941
HDL-C (mg/dl)	50.4 ± 12.6	47.1 ± 12.7	0.073	56.1 ± 15.2	52.6 ± 13.3	0.084
Triglyceride (mg/dl)	142.4 ± 64.6	163.9 ± 126.4	0.131	140.4 ± 73.9	158.7 ± 81.0	0.093
LDL-C (mg/dl)	108.0 ± 30.2	106.8 ± 24.8	0.405	101.7 ± 30.8	101.2 ± 26.2	0.915
Body Mass Index (kg/m^2)	23.9 ± 3.5	24.7 ± 3.2	0.091	23.7 ± 3.0	24.3 ± 4.3	0.270
Creatinine (mg/dl)	1.00 ± 0.41	0.99 ± 0.25	0.844	0.92 ± 0.44	0.97 ± 0.29	0.153
e-GFR (ml/min/1.73 m^2)	57.9 ± 19.2	59.6 ± 17.5	0.517			
HbA1c (%)	5.9 ± 1.2	6.1 ± 1.1	0.358	5.7 ± 0.9	5.9 ± 0.9	0.242
BNP (pg/dl)	49.8 ± 47.2	45.1 ± 29.7	0.482	46.9 ± 67.9	37.4 ± 32.3	0.211

* $p < 0.01$.
† $p < 0.05$ between baseline to follow-up.

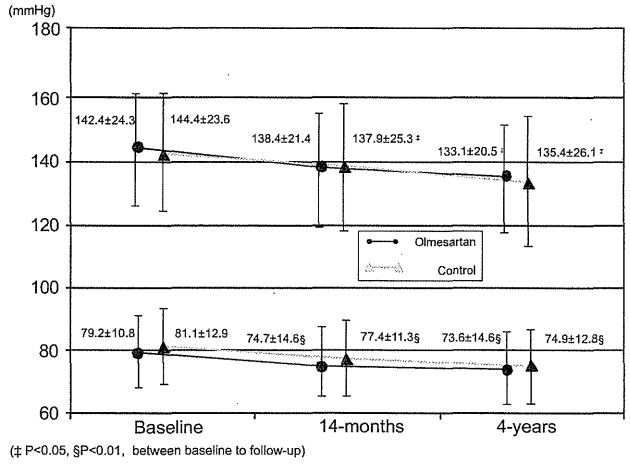

Fig. 1. Serial changes of blood pressure in the study period.

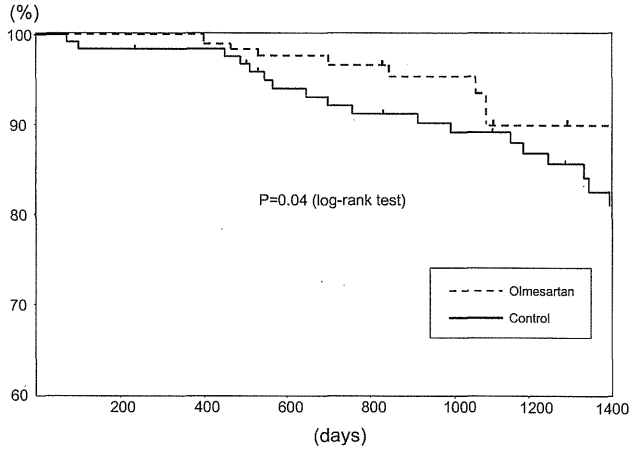

Fig. 2. Cumulative event-free from cardio or cerebrovascular death, myocardial infarction, stroke, angina, or heart/renal failure.

41.7 ± 11.5 (%), $p < 0.05$ for %ATV). However, there was no difference between ATV and %ATV in the Olmesartan group (230.2 ± 151.7 to 227.6 ± 145.8 (mm^3) for ATV, 43.8 ± 10.2 to 43.7 ± 10.4 (%) for %ATV, p = ns for all). Furthermore, serial change in ATV and %ATV were significantly lower in the Olmesartan group than in the control group (0.6 ± 12.9 vs. 5.4 ± 15.5 (%) $p = 0.016$ for ATV, −0.7 ± 13.6 vs. 3.1 ± 12.5%, $p = 0.038$ for %ATV, respectively). However, in this trial, there was no statistically significant correlation between blood pressure reduction and plaque progression rate.

3.3. *Major adverse cardio- and cerebrovascular events (MACCE)*

Adjudicated major adverse cardio- and cerebrovascular events are summarized in Table 3. While there was no difference in terms of individual cardio- and cerebrovascular event between the two groups, the composite event rate of cardio- and cerebrovascular death, MI, stroke, angina, or heart/renal failure was significantly lower in the Olmesartan group ($p = 0.041$). Cumulative event-free from MACCE was significantly higher in the Olmesartan group than in the control group ($p = 0.04$, log-rank test; Fig. 2, Hazard ratio 0.41 (95% CI: 0.18–0.91, Relative risk reduction = 0.54)). Estimates of hazard ratios for MACCE are presented in Fig. 3. Advanced age, prior history of coronary artery disease, 3-vessel disease, poorly controlled diabetes, higher %ATV increase and higher original %ATV were identified as poor predictors of MACCE. However, administration of Olmesartan and statins were selected as predictors for reduced MACCE. Comparison of serial atheroma progression rate for patients with adverse events ($n = 31$) and the rest of the population is presented in Fig. 4. Patients with adverse events had larger annual atheroma progression than the rest of the population ($p < 0.001$). During the follow-up period, there were no adverse events attributed to Olmesartan.

Table 3
Four-years adjudicated major cardiovascular events.

	Control ($n = 121$)	Olmesartan ($n = 126$)	p
Composite of cardio or cerebrovascular death, MI, stroke, angina, or heart/renal failure	17.4	8.0	0.04
Death (all cause)	3.3	3.2	0.95
Death (cardio or cerebrovascular)	1.7	0.8	0.51
Nonfatal myocardial infarction	0.8	1.6	0.59
Nonfatal stroke	1.7	0	0.15
Unstable angina/increasing angina	10.7	4.8	0.10
(Culprit related/new de novo coronary lesions)	(5.0/5.7)	(3..2/1.4)	
Deterioration of heart/renal failure	2.5	0.8	0.30

MI indicates myocardial infarction.

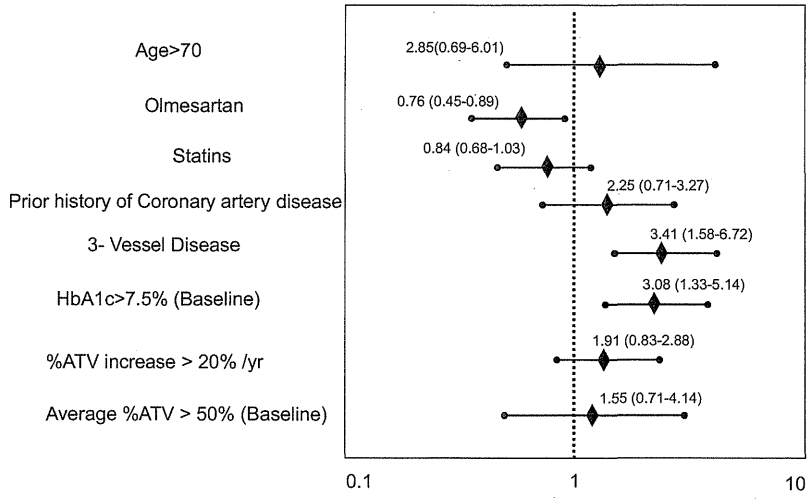

Fig. 3. Hazard ratio for major adverse cardio- and cerebrovascular events (MACCE) are presented. Hazard ratio and 95% CI value are listed.

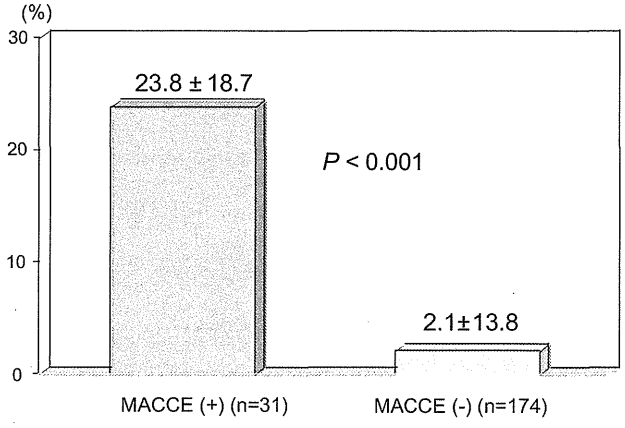

Fig. 4. Comparison of major adverse cardio- and cerebrovascular events (MACCE) and annual atheroma progression.

4. Discussion

The present study demonstrated that administration of Olmesartan was associated with reduced incidence of long-term cardio- and cerebrovascular events in patients with hypertension and stable angina pectoris after PCI. In addition, the 14-months IVUS follow-up showed that patients who had greater atheroma progression had an increase in subsequent cardio- and cerebrovascular events. In previous IVUS trials, interventions that targeted established risk factors demonstrated favorable effects on the rate of progression of coronary atherosclerosis. In the initial stage of the current trial, significant plaque regression was observed in patients receiving Olmasartan, an ARB, compared with the control group during the 14-months follow-up period. The extended-OLIVUS trial demonstrated sustained reduction in incidence of composite cardiovascular complications during the 4-years while receiving Olmesartan. Currently, ARBs are widely used for the treatment of hypertension. They also have beneficial effects on hypertension-related cardiovascular end organ damage, possibly due to reduction of oxidative stress and inflammation [19–21]. While there are several ARBs available in the clinical setting, Olmesartan is thought to have a significantly stronger antihypertensive effect than other ARBs with their respective starting doses [19–23]. In addition, previous studies as well as the OLIVUS trial have reported the potential decrease of atheromatous plaque burden in human coronary arteries after administration of Olmesartan, compared with the control group [17]. Furthermore, previous trials reported a significant reduction in the incidence of stroke and angina pectoris in patients receiving ARBs [20]. Our study data show the corroborating efficacy for these medicines in terms of preventing the progression of atherosclerosis, even though the number of enrolled patients was relatively small. However, the underlying mechanisms as well as the clinical impact of ARBs remain a matter of ongoing debate. There was no significant difference in terms of changes of blood pressure. In this trial, control of blood pressure was left to physician's discretion except for administration of ARBs and ACE inhibitors, therefore, an incremental dose of other antihypertensive agents, such as β-blockers, calcium channel blockers and/or diuretics, may have contributed to the similarities in blood pressure control between the 2 groups. In the present trial, there was no statistically significant correlation between the degree of blood pressure reduction and plaque progression rate or event rate. This may suggest the potential manifold action of Olmesartan apart from the antihypertensive effect that might be beneficial, such as activity leading to plaque stabilization and reduction. In the present trial, however, there was no significant effect on the hard events including cardiac and cerebral deaths and myocardial infarction during the 4-years follow-up period. Most events were re-hospitalizations for unstable or progressive angina, therefore, death from cardiac causes, cardiac arrest, and myocardial infarction were less common. The effects of increasing disease burden on death or myocardial infarction were not evident in this analysis, which likely reflects the finding that there were few mortal events under the current optimal medical therapy [16,24]. These results are consistent with previous trials suggesting that effects on hard endpoints using ARB showed close to the significance compared with the control group [20,23].

In the current trial, Olmesartan and statins were selected as predictors of MACCE reduction. However, a high proportion of patients in our study were showing relatively lower LDL cholesterol level at baseline, and already being treated with lipid-lowering agents (57.0% in the control and 52.3% in the Olmesartan group), which might have minimized the differences in MACCE events seen between the two randomized groups than in previous trials [1–3,5,6,9,10,12,25,26]. In the present study, it may be important to note that atheroma volume, reflecting the interaction between the artery wall and atheroma throughout the imaged segment, did associate with the likelihood of having a clinical event.

Volumetric IVUS analyses were completed exclusively in entire vessels (more than 40 mm); therefore, these IVUS parameters may represent atheroma progression of coronary as well as cerebral arteries, since atherosclerosis progresses systemically. The results suggest that atheroma volume changes, assessed by serial IVUS, seem to be a reliable surrogate for future major adverse cardio- and cerebrovascular events in this study cohort [4,12,16,17,24,27–29].

The present analysis demonstrates a relationship between the progression of coronary atherosclerosis, as determined by IVUS, and the prospective risk for cardio- and cerebrovascular events. To diminish subsequent cardiovascular risk, therapeutic strategies designed to prevent or delay the progression of coronary disease is of great clinical importance. We believe this is the first clinical trial that shows the direct potential benefits between long-term drug administration on long-term clinical outcomes and atheroma volume changes, assessed by IVUS, using an ARB. Our study data may add another striking benefit to the ever-growing list of positive outcomes associated with Olmesartan administration.

5. Limitations

There are several limitations in our study. First, a small number of patients with stable angina pectoris were enrolled; therefore, some selection bias may exist. Second, the IVUS results showed relatively larger standard deviations, however, these are not unusual for this kind of study. In addition, a high proportion of patients in our study were already being treated with optimal lipid-lowering therapy, therefore, it may be difficult to show an effect in addition to that treatment.

6. Conclusions

These observations suggest that administration of Olmesartan was associated with reduced incidence of long-term cardio- and cerebrovascular events in patients with hypertension and stable angina pectoris after PCI. Atheroma volume changes, assessed by serial IVUS, seem to be a reliable surrogate for future major adverse cardio- and cerebrovascular events in this study cohort.

Conflict of interest

None.

References

[1] Dohi T, Miyauchi K, Okazaki S, et al. Early intensive statin treatment for six months improves long-term clinical outcomes in patients with acute coronary syndrome (extended-ESTABLISH trial): a follow-up study. Atherosclerosis 2009;210:497–502.
[2] Jensen LO, Thayssen P, Pedersen KE, Stender S, Haghfelt T. Regression of coronary atherosclerosis by simvastatin: a serial intravascular ultrasound study. Circulation 2004;110:265–70.
[3] Kawasaki M, Sano K, Okubo M, et al. Volumetric quantitative analysis of tissue characteristics of coronary plaques after statin therapy using three-dimensional integrated backscatter intravascular ultrasound. J Am Coll Cardiol 2005;45:1946–53.
[4] Nicholls SJ, Hsu A, Wolski K, et al. Intravascular ultrasound-derived measures of coronary atherosclerotic plaque burden and clinical outcome. J Am Coll Cardiol 2010;55:2399–407.
[5] Nicholls SJ, Tuzcu EM, Sipahi I, et al. Statins, high-density lipoprotein cholesterol, and regression of coronary atherosclerosis. JAMA 2007;297:499–508.
[6] Nissen SE, Nicholls SJ, Sipahi I, et al. Effect of very high-intensity statin therapy on regression of coronary atherosclerosis: the ASTEROID trial. JAMA 2006;295:1556–65.
[7] Nissen SE, Nicholls SJ, Wolski K, et al. Comparison of pioglitazone vs glimepiride on progression of coronary atherosclerosis in patients with type 2 diabetes: the PERISCOPE randomized controlled trial. JAMA 2008;299:1561–73.
[8] Nissen SE, Tuzcu EM, Libby P, et al. Effect of antihypertensive agents on cardiovascular events in patients with coronary disease and normal blood pressure: the CAMELOT study: a randomized controlled trial. JAMA 2004;292:2217–25.
[9] Nissen SE, Tuzcu EM, Schoenhagen P, et al. Effect of intensive compared with moderate lipid-lowering therapy on progression of coronary atherosclerosis: a randomized controlled trial. JAMA 2004;291:1071–80.
[10] Okazaki S, Yokoyama T, Miyauchi K, et al. Early statin treatment in patients with acute coronary syndrome: demonstration of the beneficial effect on atherosclerotic lesions by serial volumetric intravascular ultrasound analysis during half a year after coronary event: the ESTABLISH Study. Circulation 2004;110:1061–8.
[11] Sarno G, Lerman A, Bae JH, et al. Multicenter assessment of coronary allograft vasculopathy by intravascular ultrasound-derived analysis of plaque composition. Nat Clin Pract Cardiovasc Med 2009;6:61–9.
[12] Nicholls SJ, Tuzcu EM, Crowe T, et al. Relationship between cardiovascular risk factors and atherosclerotic disease burden measured by intravascular ultrasound. J Am Coll Cardiol 2006;47:1967–75.
[13] Nicholls SJ, Tuzcu EM, Wolski K, et al. Coronary artery calcification and changes in atheroma burden in response to established medical therapies. J Am Coll Cardiol 2007;49:263–70.
[14] Rodriguez-Granillo GA, Agostoni P, Garcia-Garcia HM, et al. Meta-analysis of the studies assessing temporal changes in coronary plaque volume using intravascular ultrasound. Am J Cardiol 2007;99:5–10.
[15] Schartl M, Bocksch W, Koschyk DH, et al. Use of intravascular ultrasound to compare effects of different strategies of lipid-lowering therapy on plaque volume and composition in patients with coronary artery disease. Circulation 2001;104:387–92.
[16] Stone GW, Maehara A, Lansky AJ, et al. A prospective natural-history study of coronary atherosclerosis. N Engl J Med 2011;364:226–35.
[17] Hirohata A, Yamamoto K, Miyoshi T, et al. Impact of olmesartan on progression of coronary atherosclerosis a serial volumetric intravascular ultrasound analysis from the OLIVUS (impact of Olmesarten on progression of coronary atherosclerosis: evaluation by intravascular ultrasound) trial. J Am Coll Cardiol 2010;55:976–82.
[18] Nakamura M, Yock PG, Bonneau HN, et al. Impact of peri-stent remodeling on restenosis: a volumetric intravascular ultrasound study. Circulation 2001;103:2130–2.
[19] Zhang C, Hein TW, Wang W, Kuo L. Divergent roles of angiotensin II AT1 and AT2 receptors in modulating coronary microvascular function. Circ Res 2003;92:322–9.
[20] Sawada T, Yamada H, Dahlof B, Matsubara H. Effects of valsartan on morbidity and mortality in uncontrolled hypertensive patients with high cardiovascular risks: KYOTO HEART Study. Eur Heart J 2009;30:2461–9.
[21] Agata J, Ura N, Yoshida H, et al. Olmesartan is an angiotensin II receptor blocker with an inhibitory effect on angiotensin-converting enzyme. Hypertens Res 2006;29:865–74.
[22] Naya M, Tsukamoto T, Morita K, et al. Olmesartan, but not amlodipine, improves endothelium-dependent coronary dilation in hypertensive patients. J Am Coll Cardiol 2007;50:1144–9.
[23] Yusuf S, Teo K, Anderson C, et al. Effects of the angiotensin-receptor blocker telmisartan on cardiovascular events in high-risk patients intolerant to angiotensin-converting enzyme inhibitors: a randomised controlled trial. Lancet 2008;372:1174–83.
[24] Kubo T, Maehara A, Mintz GS, et al. The dynamic nature of coronary artery lesion morphology assessed by serial virtual histology intravascular ultrasound tissue characterization. J Am Coll Cardiol 2010;55:1590–7.
[25] Hartmann M, von Birgelen C, Mintz GS, et al. Relation between plaque progression and low-density lipoprotein cholesterol during aging as assessed with serial long-term (> or =12 months) follow-up intravascular ultrasound of the left main coronary artery. Am J Cardiol 2006;98:1419–23.
[26] Hartmann M, von Birgelen C, Mintz GS, Verhorst PM, Erbel R. Relation between baseline plaque burden and subsequent remodelling of atherosclerotic left main coronary arteries: a serial intravascular ultrasound study with long-term (> or =12 months) follow-up. Eur Heart J 2006;27:1778–84.
[27] von Birgelen C, Hartmann M, Mintz GS, Baumgart D, Schmermund A, Erbel R. Relation between progression and regression of atherosclerotic left main coronary artery disease and serum cholesterol levels as assessed with serial long-term (> or =12 months) follow-up intravascular ultrasound. Circulation 2003;108:2757–62.
[28] von Birgelen C, Hartmann M, Mintz GS, et al. Relationship between cardiovascular risk as predicted by established risk scores versus plaque progression as measured by serial intravascular ultrasound in left main coronary arteries. Circulation 2004;110:1579–85.
[29] Waseda K, Ozaki Y, Takashima H, et al. Impact of angiotensin II receptor blockers on the progression and regression of coronary atherosclerosis: an intravascular ultrasound study. Circ J 2006;70:1111–5.

Usefulness of the Right Parasternal Approach to Evaluate the Morphology of Atrial Septal Defect for Transcatheter Closure Using Two-Dimensional and Three-Dimensional Transthoracic Echocardiography

Nobuhisa Watanabe, RDCS, Manabu Taniguchi, MD, Teiji Akagi, MD, Yasuharu Tanabe, RDCS, Norihisa Toh, MD, Kengo Kusano, MD, Hiroshi Ito, MD, Norio Koide, MD, and Shunji Sano, MD, *Okayama, Japan*

Background: The aim of this study was to demonstrate the feasibility and usefulness of addition of the right parasternal approach to the conventional left parasternal and apical approaches using two-dimensional (2D) and three-dimensional (3D) transthoracic echocardiography (TTE) for morphologic evaluation in cases of transcatheter closure of atrial septal defects (ASDs).

Methods: In 112 consecutive patients with ASDs, the morphology of the defects was evaluated for transcatheter closure in the right parasternal view in addition to the conventional left views using 2D and 3D TTE. Measurements of the maximal ASD diameter and detection of deficient rim obtained on 2D TTE were compared with those obtained by 2D transesophageal echocardiography. The shapes and locations of ASDs visualized by 3D TTE were compared with those visualized by 3D transesophageal echocardiography.

Results: In 88 patients (80.0%), optimal images from the right parasternal approach for morphologic evaluation of ASDs were obtained. Although there was a significant difference in maximal ASD diameter obtained only in the conventional left approach compared with transesophageal echocardiographic measurements ($P < .05$), when the right parasternal approach was applied, a significant difference was not found ($P = .18$), and the diagnostic concordance of the rim deficiency was improved from 85.2% to 90.9%. Three-dimensional TTE from the right parasternal approach improved visualization of the shape and location of ASDs from 65.5% to 74.5%.

Conclusions: Additional use of the right parasternal approach enables detailed morphologic evaluation for transcatheter closure of ASDs. In patients with suboptimal images on 3D TTE in the left conventional approach, additional 3D TTE in the right parasternal approach can improve the feasibility of obtaining optimal 3D images to evaluate the shapes and locations of ASDs. (J Am Soc Echocardiogr 2012;25:376-82.)

Keywords: Right parasternal approach, Transthoracic echocardiography, Transesophageal echocardiography, Atrial septal defect

Transcatheter closure of atrial septal defects (ASDs) has recently become established as a safe and effective treatment, and the procedure has become an alternative to a surgical approach.[1-5] Appropriate patient selection for transcatheter closure is the most important factor for success in this procedure,[4] and morphologic evaluation, including evaluation of maximal ASD diameter and surrounding rims by echocardiography, is essential. Although two-dimensional (2D) transthoracic echocardiography (TTE) in the left parasternal, apical, and subcostal views is routinely used for this purpose, previous studies have demonstrated that these views enable only limited morphologic evaluation of ASDs.[6-9] Real-time three-dimensional (3D) echocardiography, in which a comprehensible en face view of ASDs is obtained, has been available in a clinical setting.[10-12] Three-dimensional TTE is expected to improve understanding of the morphology of ASDs, but data are limited, and it is difficult to obtain good-quality images on 3D TTE using the left parasternal and apical approaches.[13-15] In this regard, 2D transesophageal echocardiography (TEE) and 3D TEE have been widely accepted and established as diagnostic modalities in evaluation of the morphology of ASDs for transcatheter closure because of their high-quality imaging[16-21]; however, TEE has a semi-invasive nature.

The right parasternal approach, in which the transducer is placed to the right of the sternum in the right lateral decubitus position, was

From the Division of Medical Support (N.W., Y.T.) and the Division of Cardiac Intensive Care Unit (M.T., T.A.), Okayama University Hospital, Okayama, Japan; the Department of Cardiovascular Medicine (N.T., K.K., H.I.), the Department of Laboratory Medicine (N.K.), and the Department of Cardiovascular Surgery (S.S.), Okayama University Graduate School of Medicine, Dentistry and Pharmaceutical Sciences, Okayama, Japan.

Reprint requests: Manabu Taniguchi, MD, 2-5-1 Kita-ku Shikata-Cho, Okayama 700-8558, Japan (E-mail: *tmnb@md.okayama-u.ac.jp*).

0894-7317/$36.00

doi:10.1016/j.echo.2012.01.002

Abbreviations

ASD = Atrial septal defect

TEE = Transesophageal echocardiography

3D = Three-dimensional

TTE = Transthoracic echocardiography

2D = Two-dimensional

reported to enable better visualization of ASDs and evaluation of the direction of shunt flow in patients with ASDs because it obtains a longitudinal vena cava superior-inferior plane of the interatrial septum.[22-26] In addition, 3D TTE in this approach might improve the feasibility of obtaining optimal en face images of ASDs. However, there have been limited data on the usefulness of the right parasternal approach using 2D and 3D TTE for morphologic evaluation in cases of transcatheter closure. Therefore, we sought to assess the usefulness of the right parasternal approach in addition to the conventional left parasternal and apical approaches in evaluating ASD morphology for the suitability of transcatheter closure using 2D and 3D TTE.

METHODS

Study Population

A total of 112 consecutive patients (40 men and 72 women) were prospectively evaluated for transcatheter closure of ASDs using the Amplatzer Septal Occluder (AGA Medical Corporation, Plymouth, MN) with 2D and 3D TTE. Two patients with ASDs other than the secundum type were excluded from this study (one had a superior sinus venosus ASD and the other had an unroofed coronary sinus ASD). Therefore, 110 patients were included in the study. All patients except for one were referred from other hospitals to our institution for transcatheter ASD closure. Age at the examination ranged from 6 to 84 years (mean, 46.1 ± 20.5 years). Two-dimensional TEE and 3D TEE were performed <3 days after TTE by a blinded observer. The study was approved by the local ethics committee.

Two-Dimensional TTE

Two-dimensional TTE was performed using a commercially available ultrasound system with a 3.5-MHz transducer (Vivid 7; GE Healthcare, Wauwatosa, WI). Right ventricular midcavity diameter was measured in the apical four-chamber view according to the guideline of American Society of Echocardiography.[27] In all patients, the morphology of ASDs was evaluated using TTE in the left lateral decubitus position from the left parasternal and apical approaches (conventional left approach). Then a transducer was positioned on the right parasternal border with the patient in the right lateral decubitus position (right parasternal approach). Maximal ASD diameter and the minimal diameter of surrounding rims were measured at end-systole by carefully sweeping the transducer from right to left and top to bottom of the interatrial septum in both approaches. Regarding the maximal ASD diameter, first, the ASD diameter was measured using the conventional left approach (ASD_L diameter), and then the ASD diameter was measured by the right parasternal approach (ASD_R diameter). The maximal ASD diameter was considered the maximal value from measurements by both approaches. The surrounding rims were classified according to location as superoanterior, inferoanterior, superoposterior, or inferoposterior. The superoanterior rim was measured as the distance between the aorta and the defect. The inferoanterior rim was measured as the distance from the atrioventricular valves. The inferoposterior rim was measured as the distance from the left atrial wall. The superoposterior rim was measured as the distance from the defect to the superior vena cava and to determine the inferoposterior rim as the distance from the defect to the inferior vena cava (Figure 1). Any rim length < 5 mm was considered deficient. First, the presence or absence of a deficient rim was evaluated using the conventional left approach, and then the right parasternal approach was used.

Three-Dimensional TTE

Three-dimensional TTE was performed after 2D TTE using a commercially available ultrasound system with a 3V transducer (Vivid 7). In all patients, the left parasternal approach was first chosen and optimized, and then loops from five consecutive cycles were acquired and digitally stored. In cases with suboptimal 3D images by the left parasternal approach, we attempted to obtain optimal 3D images using the right parasternal approach. In all patients, at least three acquisitions were performed, and the data set with the best image quality was chosen for analysis. The shapes and locations of ASDs were visually evaluated on the best 3D images.

Two-Dimensional and 3D TEE

Two-dimensional and 3D TEE were performed using a commercially available ultrasound system (iE33; Philips Medical Systems, Andover, MA). Maximal ASD diameter (ASD_{TEE} diameter) and minimal diameter of the surrounding rims were assessed at end-systole using both 2D TEE and 3D TEE, as previously reported.[18] To evaluate surrounding rims using 2D TEE, the superoanterior rim was measured as the distance between the aortic annulus and the defect in the horizontal plane at 0° to 30°. The inferoanterior rim was measured as the distance between the defect and atrioventricular valves in the four-chamber view at 135°. The longitudinal plane around 90° was used to determine the superoposterior rim as the distance from the defect to the superior vena cava and to determine the inferoposterior rim as the distance from the defect to the inferior vena cava (Figure 1). The rim length was considered deficient if the length was <5 mm.

Real-time 3D transesophageal echocardiographic data were obtained after a complete 2D transesophageal echocardiographic study. Real-time 3D zoom mode, which displays a smaller, magnified pyramidal data set, was used to evaluate the shapes and locations of ASDs as well as the rough relation to surrounding structures.

Two-dimensional and 3D transesophageal echocardiographic data were considered reference standards. In patients with optimal images obtained on both approaches, ASD_{TEE} diameter and detection of deficient rims obtained on 2D TEE were compared with those obtained on 2D TTE. The shapes and locations of ASDs using 3D TTE were compared with those obtained using 2D and 3D TEE.

Measurement Variability

ASD diameter and the minimal diameter of the surrounding rims obtained using TTE were measured by two independent observers and by one observer two times 1 month apart in 10 randomly selected patients to determine interobserver variability and intraobserver variability. Variability was assessed as the absolute difference between two measurements expressed as a percentage of their mean values.

Statistical Analysis

Categorical data are expressed as numbers and percentages and continuous data as mean ± SD. The significance of baseline differences

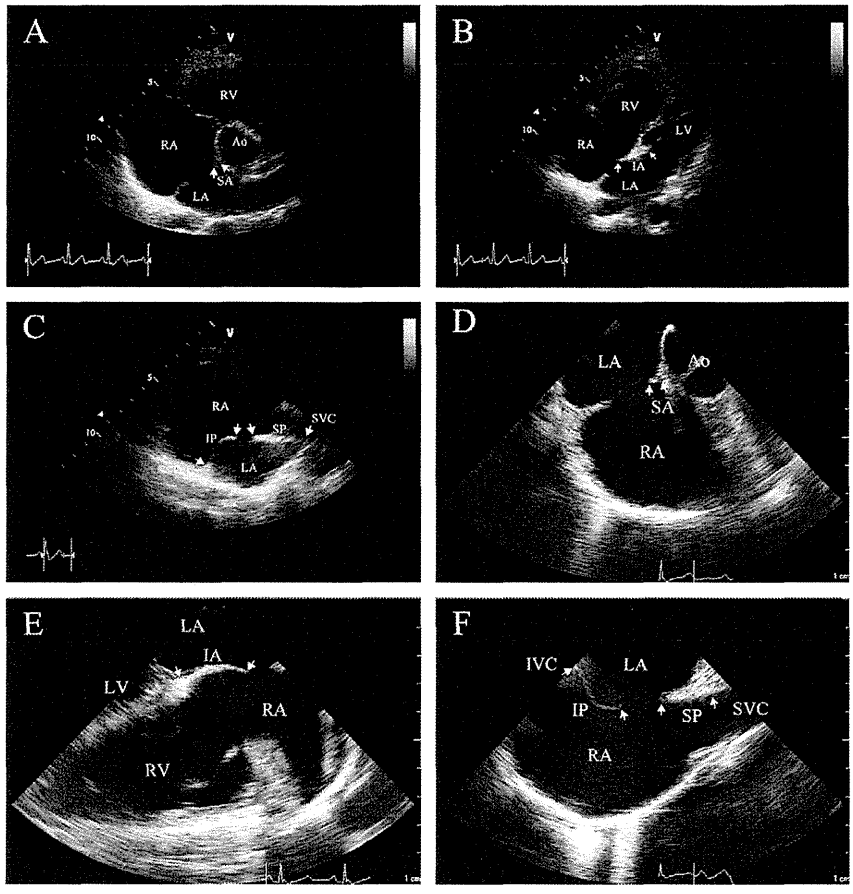

Figure 1 Measurement of maximal ASD diameter and the surrounding rims on 2D TTE and 2D TEE. The surrounding rim is measured from mark (*white arrow*) to mark (*white arrow*). **(A)** Left parasternal short-axis view, **(B)** left parasternal four-chamber view, **(C)** right parasternal longitudinal view, **(D)** short-axis transesophageal echocardiographic view (0°–30°), **(E)** four-chamber transesophageal echocardiographic view (135°), **(F)** biatrial transesophageal echocardiographic view (90°). The surrounding rims are measured at end-systole (*white arrow*). *Ao*, Aorta; *IA*, inferoanterior rim; *IP*, inferoposterior rim; *IVC*, inferior vena cava; *LA*, left atrium; *LV*, left ventricle; *RA*, right atrium; *RV*, right ventricle; *SA*, superoanterior rim; *SP*, superoposterior rim; *SVC*, superior vena cava.

was determined using paired and unpaired *t* tests as appropriate. Categorical variables are expressed as counts and percentages and were compared using χ^2 or Fisher's exact tests as appropriate. Comparisons between measurements were done using Pearson's linear regressions analysis. The agreement of the two methods was evaluated using the Bland-Altman test. *P* values $< .05$ were considered statistically significant. Statistical analyses were done using SPSS version 18.0 (SPSS, Inc., Chicago, IL).

RESULTS

Baseline Characteristics of Study Population

Table 1 shows the baseline characteristics and 2D transthoracic echocardiographic parameters of the study population. All patients showed hemodynamically significant atrial shunts or the presence of right atrial and ventricular volume overload.

Feasibility of 2D TTE in the Right Parasternal Approach

Two-dimensional TTE with the conventional left approach enabled the detection of shunt flow on color-flow Doppler imaging and visualization of the optimal images for the measurement of defects in all patients. Detection of shunt flow in the right parasternal approach on color-flow Doppler images was successful in 102 patients (92.7%). Optimal images with the right parasternal approach for measurements of defects and surrounding rims were visualized in 88 patients (80.0%). When all patients were divided into two groups according to age, <40 years ($n = 42$; mean age, 24.1 ± 10.4 years) and ≥40 years ($n = 68$; mean age, 59.6 ± 11.5 years), the percentage of patients in whom optimal images to measure ASD diameter and surrounding

Table 1 Baseline characteristics and transthoracic echocardiographic parameters of the study population ($n = 110$)

Variable	Value
Men/women	39/71
Age (y)	46.1 ± 20.5 (6–84)
Height (m)	1.58 ± 0.12 (1.13–1.83)
Weight (kg)	54 ± 12.3 (17–92)
Body surface area (m^2)	1.53 ± 0.22 (0.75–2.14)
Right ventricular midcavity diameter (mm)	41.8 ± 5.4 (28–55)
Pulmonary flow/systemic flow ratio	2.4 ± 0.7 (1.2–4.1)

Data are expressed as numbers or as mean ± SD (range).

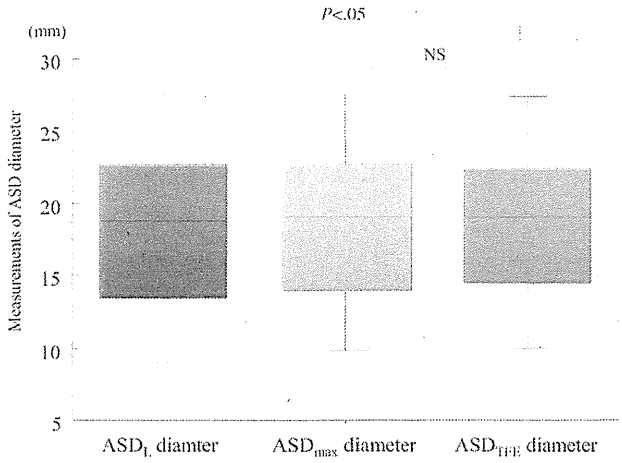

Figure 2 Box plots showing the comparison ASD_L diameter obtained with the conventional left approach (*red box*), maximal ASD diameter obtained with both the left conventional and right parasternal approaches (*orange box*), and ASD_{TEE} diameter (*blue box*).

rim were obtained in the right parasternal approach was significantly higher in those aged <40 years than in those aged ≥40 years (90.5% vs 73.5%, $P = .033$).

Data for the 88 patients in whom optimal 2D transthoracic echocardiographic images for measurements of ASD diameter and surrounding rims were obtained by both approaches were analyzed in our study.

Morphologic Evaluation with 2D TTE and TEE

Maximal ASD diameters between ASD_L diameter, maximal ASD diameter, and ASD_{TEE} diameter were compared in 88 patients with optimal images from the right parasternal approach. There was a small but significant difference between ASD_L diameter and ASD_{TEE} diameter (18.5 ± 6.9 vs 19.0 ± 6.9 mm, $P < .05$). However, when the diameter obtained with the right parasternal approach was taken into account in addition to the diameter obtained with the conventional left approach, a significant difference was not found between measurements of maximal ASD diameter and ASD_{TEE} diameter (18.8 ± 6.7 mm, $P = .18$; Figure 2). Bland-Altman analysis showed the smallest mean absolute differences and narrower limits of agreement when the measurement from the right parasternal approach was added to that from the conventional left approach (Figure 3).

TEE demonstrated that 17 patients (19.3%) had centrally positioned ASD, 55 (62.5%) had superoanterior rim deficiencies, three (3.4%) had inferoposterior deficiencies, five (5.7%) had both superoanterior and inferoposterior deficiencies, and eight (9.1%) had multiple ASDs. Although the detection of a deficient rim showed concordance in 75 patients (85.2%) between TTE with the conventional left approach and 2D TEE, diagnostic concordance was improved to 90.9% by adding the right parasternal approach. In nine patients with inferoposterior rim deficiencies, diagnostic accuracy of the rim deficiency was improved from 66.7% to 100% when the right parasternal approach was added to the conventional left approach.

Evaluation of ASDs with 3D TTE

Although 3D TTE from the left parasternal approach could visualize the 3D optimal image for understanding the shape and location of

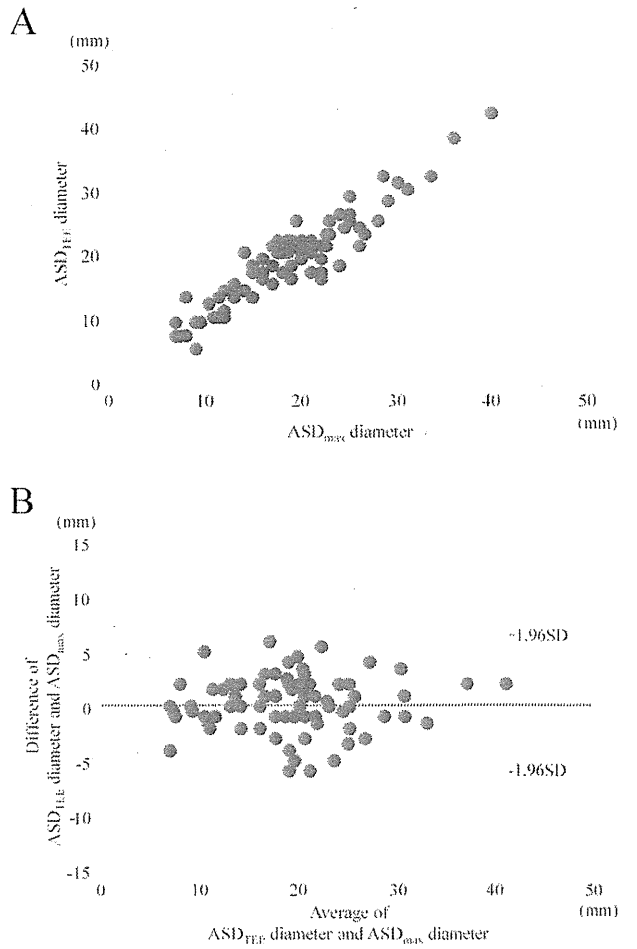

Figure 3 **(A)** Correlations of maximal ASD diameter measured by 2D TTE versus 2D TEE. **(B)** Bland-Altman plot of ASD diameter difference between the measurements on 2D TTE and those on 2D TEE as a function of the average measurements. The *thick continuous line* and *dotted line* indicate the mean ± 1.96 SD of the difference, respectively.

ASDs in only 72 patients (65.5%), the use of the right parasternal approach improved the visualization of optimal 3D TTE images to 74.5% (Figures 4 and 5).

Measurement Variability

Interobserver and intraobserver variability were 1.1% and 0.6%, respectively, for ASD diameter measured by 2D TTE; 6.1% and 6.8%, respectively, for superoposterior rim measurement by 2D TTE; and 9.7% and 8.0%, respectively, for inferoposterior rim measurement by 2D TTE.

DISCUSSION

Our study demonstrated that 2D TTE with the addition of the right parasternal approach to the conventional left approach is feasible and enables evaluation of the morphology of ASDs for transcatheter closure with satisfactory accuracy compared with evaluation by 2D TEE. In particular, the right parasternal approach contributes greatly

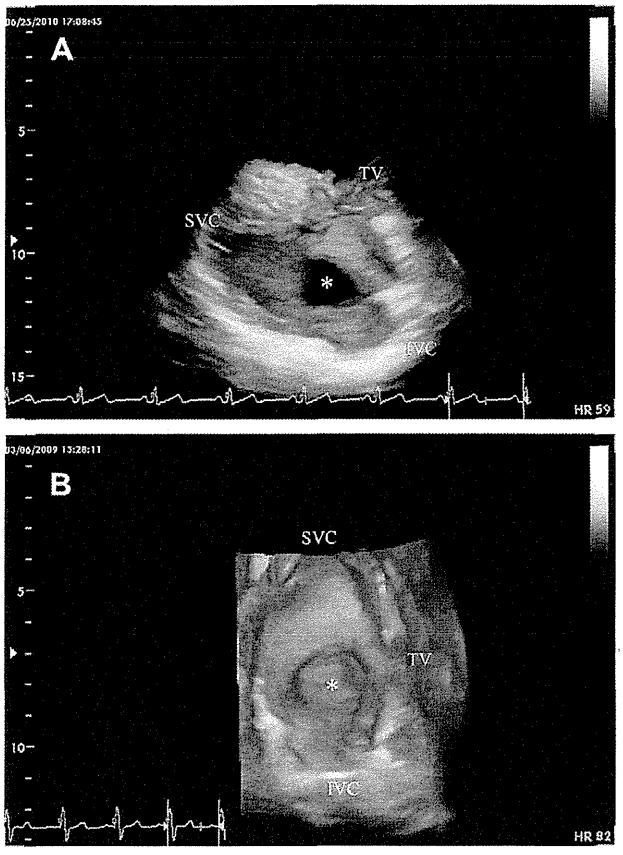

Figure 4 Three-dimensional transthoracic echocardiography of various shapes of the secundum-type ASD (*asterisk*) viewed from the right atrium. **(A)** Superoanterior rim deficient from the left parasternal approach, **(B)** inferoposterior rim deficient from the right parasternal approach. *IVC*, Inferior vena cava; *SVC*, superior vena cava; *TV*, tricuspid valve.

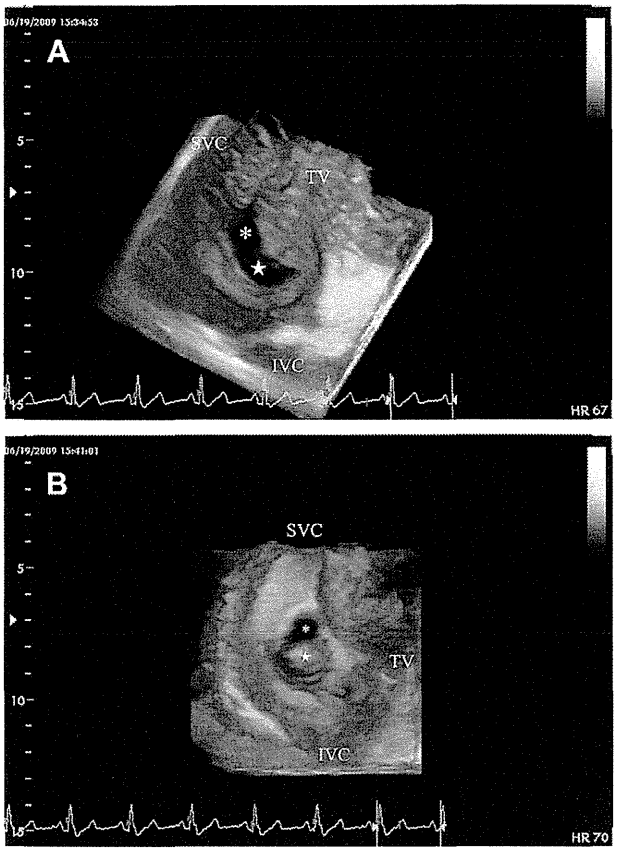

Figure 5 Three-dimensional TTE of the secundum-type ASD (*asterisk*) with an atrial septal aneurysmal (ASA) viewed from the right atrium. **(A)** The ASA (*white star*) was dropped out from the left parasternal approach **(B)** but was clearly visualized from the right parasternal approach. *IVC*, Inferior vena cava; *SVC*, superior vena cava; *TV*, tricuspid valve.

to the identification of rim deficiency, especially in patients with inferoposterior rim deficiencies. In terms of the acquisition of optimal 3D transthoracic echocardiographic images, the addition of the right parasternal approach to the conventional left approach can improve the feasibility of ASD morphologic evaluation.

Feasibility of the Right Parasternal Approach

Previous studies have shown that the right parasternal approach is a reliable technique for detection of ASDs.[22-26] Iliceto *et al.*[25] reported that ASDs were identified using the right parasternal approach in 13 of 17 patients (76.5%) and that the right parasternal approach improved the feasibility of 2D TTE for the detection of ASDs. In our study, we could detect ASDs on color-flow Doppler imaging by 2D TTE using the right parasternal approach with high sensitivity (92.7%). Advances in the technology of echocardiography may have greatly contributed to its high feasibility compared with previous studies. In our study, optimal images in the right parasternal approach were obtained more frequently in younger patients than in older patients, who sometimes have obesity or lung disease. A previous study also demonstrated that the right parasternal view was often easily obtainable in neonates and young children.[26] Therefore, especially in younger patients with intolerance of TEE, TTE including the right parasternal approach can contribute to evaluating ASD morphology for transcatheter closure.

Morphologic Evaluation of ASDs

Previous studies have demonstrated that appropriate patient selection is essential for successful transcatheter closure of ASDs using the Amplatzer Septal Occluder.[16,17] Two crucial parameters, maximal ASD diameter to choose an appropriately sized device and tissue rim dimensions all around the defect to optimize placement of the device, should be measured to select patients for transcatheter closure of ASDs in addition to detection of atrial shunts or echocardiographic findings of right ventricular volume overload.[12] Although TEE is considered the gold standard in evaluating ASD morphology for the suitability of transcatheter closure, TEE has a semi-invasive nature. TTE used to perform a detailed morphologic evaluation of ASDs before TEE can lead to avoiding oversight and shortening transesophageal examination time. Therefore, detailed morphologic evaluation, including evaluation of maximal ASD diameter and surrounding rims by TTE, is important. In our study, the use of the additional right parasternal approach in TTE improved measurements of maximal ASD diameter and detection of rim deficiencies and enabled morphologic evaluation comparable with that obtained by TEE. In the conventional left approach, because the

direction of the ultrasound beam is almost parallel to the interatrial septum, there is frequent dropout of interatrial septal echoes in the region of the mid portion (fossa ovalis). Previous studies have shown that echo dropout in the region of the mid portion frequently occurs and can lead to false diagnoses of large defects.[22,28,29] One of those previous studies showed that the maximal ASD diameter measured with 2D TTE was larger than that measured with 2D TEE and that there was a poor correlation between these measurements because of dropout in the region of the fossa ovalis.[29] The subcostal approach is another useful method for visualizing perpendicularly the interatrial septum.[28] Although 2D TTE from the subcostal approach enables the detection of shunt flow across ASDs easily in pediatric patients,[25,28] this approach can provide suboptimal images or incomplete clinical information with regard to morphologic evaluation for transcatheter ASDs closure, especially in adult patients, because of the limited echocardiographic window.[6-8] The right parasternal approach is a method that can provide better evaluation of the structure of the interatrial septal because the ultrasound beam passes in a plane perpendicular to the interatrial septal.[22-26] The use of the right parasternal approach provided better visualization of the superior vena cava and inferior vena cava entering into the right atrium. The right parasternal approach contributed greatly to the detection of deficient rims in the present study, particularly for the inferoposterior rim, which is sometimes difficult to visualize clearly by TEE. A previous study showed that inferior rim deficiency was a significant factor associated with unsuccessful transcatheter closure.[30] Therefore, the additional right parasternal view can contribute to appropriate patient selection and the prediction of procedural results for transcatheter ASD closure.

Considerable experience and operator skills are necessary for evaluating ASD morphology precisely using 2D TTE, equivalent to 2D TEE. There are some issues of technique and some pitfalls. The ultrasound beam should be passed as perpendicularly to the interatrial septum as possible. In addition, gain adjustment using time-gain compensation, focus position, and the use of zoom mode (high frame rate) should be set for morphologic evaluation. In addition, control of respiration and body position should be required to avoid potential artifacts such as dropout and side lobe.

Three-Dimensional Echocardiography Using the Right Parasternal Approach

ASDs are known to have complex geometry that may be elliptical, ovoid, or multiple defects or fenestrations.[20,21] Three-dimensional echocardiography provides more spatial anatomic information without the need for mental 2D reconstruction. There have been several studies on the usefulness for assessing ASDs of 3D transesophageal echocardiographic reconstruction[10-12] and real-time 3D TEE.[18-21] In addition, some previous studies have demonstrated possible usefulness of 3D TTE for evaluating ASD morphology.[18,21,22] Acar *et al.*[31] reported a high correlation between 3D transthoracic and 3D transesophageal echocardiographic measurements of maximal ASD diameter in pediatric patients. Van den Bosch *et al.*[13] demonstrated that real-time 3D TTE enabled reliable assessment of the dimensions of ASDs and the exact location and extent of the surrounding rim, and they reported an excellent correlation of real-time 3D transthoracic echocardiographic findings compared with surgical and 2D transesophageal echocardiographic measurements of ASDs in pediatric and relatively young adult patients. Chen *et al.*[14] reported that 3D TTE could provide accurate diagnosis of sinus venosus ASDs. In terms of the usefulness of 3D TTE in the right parasternal approach for evaluating ASD morphology, although there was one case report, studies with a sufficient number patients and including patients with a wide age range have been limited. In the present study, we demonstrated that the use of the right parasternal approach in addition to the conventional left approach improved the feasibility of visualization of satisfactory 3D images, even in adult patients.

Limitations

This study had some limitations. First, the number of patients in this study was relatively small to conclude whether the extent of variation in ASD type was taken into account. Second, almost all patients in the present study were referred from other hospitals to our institution for transcatheter closure of ASDs. Therefore, patient selection bias could have existed before enrollment. Third, visualizing ASDs and surrounding rims using the right parasternal approach requires a learning curve. In this study, interobserver variability and intraobserver variability were quantitatively evaluated by two skilled operators. Finally, evaluation in the subcostal view may improve the feasibility and accuracy of TTE.

CONCLUSIONS

The use of the right parasternal approach enables detailed morphologic evaluation, especially for longitudinal ASD diameter, superoanterior rim diameter, and inferoposterior rim diameter of ASDs in a longitudinal vena cava superior-inferior plane of the interatrial septum. In patients with suboptimal images with the conventional left approach, additional 3D TTE in the right parasternal approach can improve the feasibility of obtaining optimal 3D images to evaluate the shapes and locations of ASDs.

REFERENCES

1. Butera G, Romagnoli E, Carminati M, Chessa M, Piazza L, Negura D, et al. Treatment of isolated secundum atrial septal defects: impact of age and defect morphology in 1,013 consecutive patients. Am Heart J 2008;156:706-12.
2. Chessa M, Carminati M, Butera G, Bini RM, Drago M, Rosti L, et al. Early and late complications associated with transcatheter occlusion of secundum atrial septal defect. J Am Coll Cardiol 2002;39:1061-5.
3. Berger F, Ewert P, Björnstad PG, Dähnert I, Krings G, Brilla-Austenat I, et al. Transcatheter closure as standard treatment for most interatrial defects: experience in 200 patients treated with the Amplatzer Septal Occluder. Cardiol Young 1999;9:468-73.
4. Du ZD, Hijazi ZM, Kleinman CS, Silverman NH, Larntz K. Amplatzer nvestigators. Comparison between transcatheter and surgical closure of secundum atrial septal defect in children and adults: results of a multicenter nonrandomized trial. J Am Coll Cardiol 2002;39:1836-44.
5. Thomson JD, Aburawi EH, Watterson KG, Van Doorn C, Gibbs JL. Surgical and transcatheter (Amplatzer) closure of atrial septal defects: a prospective comparison of results and cost. Heart 2002;87:466-9.
6. Hanrath P, Schlüter M, Langenstein BA, Polster J, Engel S, Kremer P, et al. Detection of ostium secundum atrial septal defects by transoesophageal cross-sectional echocardiography. Br Heart J 1983;49:350-8.
7. Morimoto K, Matsuzaki M, Tohma Y, Ono S, Tanaka N, Michishige H, et al. Diagnosis and quantitative evaluation of secundum-type atrial septal defect by transesophageal Doppler echocardiography. Am J Cardiol 1990;66:85-91.
8. Kronzon I, Tunick PA, Freedberg RS, Trehan N, Rosenzweig BP, Schwinger ME. Transesophageal echocardiography is superior to

transthoracic echocardiography in the diagnosis of sinus venosus atrial septal defect. J Am Coll Cardiol 1991;17:537-42.
9. Mehta RH, Helmcke F, Nanda NC, Pinheiro L, Samdarshi TE, Shah VK. Uses and limitations of transthoracic echocardiography in the assessment of atrial septal defect in the adult. Am J Cardiol 1991;67:288-94.
10. Tamborini G, Pepi M, Susini F, Trabattoni D, Maltagliati A, Berna G, et al. Comparison of two- and three-dimensional transesophageal echocardiography in patients undergoing atrial septal closure with the Amplatzer Septal Occluder. Am J Cardiol 2002;90:1025-8.
11. Pepi M, Tamborini G, Bartorelli AL, Trabattoni D, Maltagliati A, De Vita S, et al. Usefulness of three-dimensional echocardiographic reconstruction of the Amplatzer Septal Occluder in patients undergoing atrial septal closure. Am J Cardiol 2004;94:1343-7.
12. Acar P, Saliba Z, Bonhoeffer P, Aggoun Y, Bonnet D, Sidi D, et al. Influence of atrial septal defect anatomy in patient selection and assessment of closure with the Cardioseal device; a three-dimensional transoesophageal echocardiographic reconstruction. Eur Heart J 2000;21:573-81.
13. Van den Bosch AE, Ten Harkel DJ, McGhie JS, Roos-Hesselink JW, Simoons ML, Bogers AJ, et al. Characterization of atrial septal defect assessed by real-time 3-dimensional echocardiography. J Am Soc Echocardiogr 2006;19:815-21.
14. Chen CA, Wang JK, Hsu JY, Hsu HH, Chen SJ, Wu MH. Diagnosis of inferior sinus venosus atrial septal defects using transthoracic three-dimensional echocardiography. J Am Soc Echocardiogr 2009;23:457.e4-6.
15. Mehmood F, Vengala S, Nanda NC, Dod HS, Sinha A, Miller AP, et al. Usefulness of live three-dimensional transthoracic echocardiography in the characterization of atrial septal defects in adults. Echocardiography 2004;21:707-13.
16. Mazic U, Gavora P, Masura J. The role of transesophageal echocardiography in transcatheter closure of secundum atrial septal defects by the Amplatzer Septal Occluder. Am Heart J 2001;142:482-8.
17. Prokselj K, Kozelj M, Zadnik V, Podnar T. Echocardiographic characteristics of secundum-type atrial septal defects in adult patients: implications for percutaneous closure using Amplatzer Septal Occluders. J Am Soc Echocardiogr 2004;17:1167-72.
18. Taniguchi M, Akagi T, Watanabe N, Okamoto Y, Nakagawa K, Kijima Y, et al. Application of real-time three-dimensional transesophageal echocardiography using a matrix array probe for transcatheter closure of atrial septal defect. J Am Soc Echocardiogr 2009;22:1114-20.
19. Kijima Y, Taniguchi M, Akagi T, Nakagawa K, Kusano K, Ito H, et al. Torn atrial septum during transcatheter closure of atrial septal defect visualized by real-time three-dimensional transesophageal echocardiography. J Am Soc Echocardiogr 2010;23:1222.e5-8.
20. Lodato JA, Cao QL, Weinert L, Sugeng L, Lopez J, Lang RM, et al. Feasibility of real-time three-dimensional transoesophageal echocardiography for guidance of percutaneous atrial septal defect closure. Eur J Echocardiogr 2009;10:543-8.
21. Johri AM, Witzke C, Solis J, Palacios IF, Inglessis I, Picard MH, et al. Real-time three-dimensional transesophageal echocardiography in patients with secundum atrial septal defects: outcomes following transcatheter closure. J Am Soc Echocardiogr 2011;24:431-7.
22. Tei C, Tanaka H, Kashima T, Yoshimura H, Minagoe S, Kanehisa T. Real-time cross-sectional echocardiographic evaluation of the interatrial septum by right atrium-interatrial septum-left atrium direction of ultrasound beam. Circulation 1979;60:539-46.
23. Minagoe S, Tei C, Kisanuki A, Arikawa K, Nakazono Y, Yoshimura H, et al. Noninvasive pulsed Doppler echocardiographic detection of the direction of shunt flow in patients with atrial septal defect: usefulness of the right parasternal approach. Circulation 1985;71:745-53.
24. McDonald RW, Rice MJ, Reller MD, Marcella CP, Sahn DJ. Echocardiographic imaging techniques with subcostal and right parasternal longitudinal views in detecting sinus venosus atrial septal defects. J Am Soc Echocardiogr 1996;9:195-8.
25. Iliceto S, Antonelli G, Sorino M, Ricci A. Detection of atrial septal defect by right sternal border echocardiography. Am J Cardiol 1984;54:376-8.
26. Luckie M, Buckley H, Khattar R. Echocardiographic detection of atrial septal defects: the forgotten view. Echocardiography 2010;27:97-9.
27. Rudski LG, Lai WW, Afilalo J, Hua L, Handschumacher MD, Chandrasekaran K, et al. Guidelines for the echocardiographic assessment of the right heart in adults: a report from the American Society of Echocardiography endorsed by the European Association of Echocardiography, a registered branch of the European Society of Cardiology, and the Canadian Society of Echocardiography. J Am Soc Echocardiogr 2010;23:685-713.
28. Shub C, Dimopoulos IN, Seward JB, Callahan JA, Tancredi RG, Schattenberg TT, et al. Sensitivity of two-dimensional echocardiography in the direct visualization of atrial septal defect utilizing the subcostal approach: experience with 154 patients. J Am Coll Cardiol 1983;2:127-35.
29. Konstantinides S, Kasper W, Geibel A, Hofmann T, Köster W, Just H. Detection of left-to-right shunt in atrial septal defect by negative contrast echocardiography: a comparison of transthoracic and transesophageal approach. Am Heart J 1993;126:909-17.
30. Varma C, Benson LN, Silversides C, Yip J, Warr MR, Webb G, et al. Outcomes and alternative techniques for device closure of the large secundum atrial septal defect. Catheter Cardiovasc Interv 2004;61:131-9.
31. Acar P, Dulac Y, Roux D, Rougé P, Duterque D, Aggoun Y. Comparison of transthoracic and transesophageal three-dimensional echocardiography for assessment of atrial septal defect diameter in children. Am J Cardiol 2003;91:500-2.

International Journal of Cardiology 159 (2012) 100–106

Contents lists available at SciencesDirect

International Journal of Cardiology

journal homepage: www.elsevier.com/locate/ijcard

Pro-apoptotic effects of imatinib on PDGF-stimulated pulmonary artery smooth muscle cells from patients with idiopathic pulmonary arterial hypertension ☆

Kazufumi Nakamura [a,*], Satoshi Akagi [a], Aiko Ogawa [a], Kengo F. Kusano [a], Hiromi Matsubara [b], Daiji Miura [a], Soichiro Fuke [a], Nobuhiro Nishii [a], Satoshi Nagase [a], Kunihisa Kohno [a], Hiroshi Morita [a], Takahiro Oto [c], Ryutaro Yamanaka [d], Fumio Otsuka [d], Aya Miura [a], Chikao Yutani [e], Tohru Ohe [a], Hiroshi Ito [a]

[a] Department of Cardiovascular Medicine, Okayama University Graduate School of Medicine, Dentistry and Pharmaceutical Sciences, Okayama, Japan
[b] Division of Cardiology, National Hospital Organization Okayama Medical Center, Okayama, Japan
[c] Department of Cancer and Thoracic Surgery, Okayama University, Okayama, Japan
[d] Department of Medicine and Clinical Science, Okayama University, Okayama, Japan
[e] Department of Life Science, Okayama University of Science, Okayama, Japan

ARTICLE INFO

Article history:
Received 16 September 2010
Received in revised form 11 January 2011
Accepted 7 February 2011
Available online 4 March 2011

Keywords:
Apoptosis
Hypertension
Pulmonary
Remodeling

ABSTRACT

Background: Remodeling of the pulmonary artery by an inappropriate increase of pulmonary artery smooth muscle cells (PASMCs) is problematic in the treatment of idiopathic pulmonary arterial hypertension (IPAH). Effective treatment that achieves reverse remodeling is required. The aim of this study was to assess the pro-apoptotic effects of imatinib, a platelet-derived growth factor (PDGF)-receptor tyrosine kinase inhibitor, on PASMCs obtained from patients with IPAH.

Methods: PASMCs were obtained from 8 patients with IPAH undergoing lung transplantation. Cellular proliferation was assessed by ^{3}H-thymidine incorporation. Pro-apoptotic effects of imatinib were examined using TUNEL and caspase-3,7 assays and using transmission electron microscopy.

Results: Treatment with imatinib (0.1 to 10 μg/mL) significantly inhibited PDGF-BB (10 ng/mL)-induced proliferation of PASMCs from IPAH patients. Imatinib (1 μg/mL) did not induce apoptosis in quiescent IPAH-PASMCs, but it had a pro-apoptotic effect on IPAH-PASMCs stimulated with PDGF-BB. Imatinib did not induce apoptosis in normal control PASMCs with or without PDGF-BB stimulation. PDGF-BB induced phosphorylation of Akt at 15 min, and Akt phosphorylation was inhibited by imatinib in IPAH-PASMCs. Akt-I-1/2 (1 μmol/L), an Akt inhibitor, in the presence of PDGF-BB significantly increased apoptotic cells compared with the control condition. Thus, Akt-I-1/2 could mimic the effects of imatinib on PASMCs.

Conclusion: Imatinib has anti-proliferative and pro-apoptotic effects on IPAH-PASMCs stimulated with PDGF. The inhibitory effect of imatinib on Akt phosphorylation induced by PDGF plays an important role in the pro-apoptotic effect.

1. Introduction

Idiopathic pulmonary arterial hypertension (IPAH) is a progressive disease characterized by progressive elevation of pulmonary vascular resistance and pulmonary artery pressure. Increased pulmonary vascular resistance is induced by pulmonary vasoconstriction, vascular remodeling by intimal and medial hypertrophy, and thrombosis [1,2]. Pulmonary vascular medial hypertrophy is caused by an inappropriate increase in pulmonary artery smooth muscle cells (PASMCs). Treatment with several vasodilators such as calcium channel blockers, prostaglandin I_2 and endothelin receptor antagonists was found to improve survival of patients with IPAH, but 5-year survival remains at 50% [3,4]. Effective treatment that achieves reverse remodeling is needed. This will require anti-proliferative and pro-apoptotic agents for PASMCs.

We have reported that platelet-derived growth factor (PDGF)-BB stimulation causes a higher growth rate of cultured PASMCs from patients with IPAH than that of control cells [5–7]. Recently, the use of a PDGF-receptor inhibitor such as imatinib (STI571) is starting to garner attention as a targeted therapy for pulmonary hypertension (PH) [8–11]. Imatinib is a drug used to treat certain types of cancer such as chronic myelogenous leukemia and gastrointestinal stromal tumors. In laboratory settings, imatinib is used as an experimental agent to suppress PDGF by inhibiting PDGF receptor ß (PDGF-Rß). It is an agent that acts by specifically inhibiting a certain enzyme, tyrosine kinase, that

☆ Dr. Nakamura was supported by the Research Grant for Cardiovascular Diseases (19–9) from the Ministry of Health, Labour and Welfare, Japan.

* Corresponding author at: Department of Cardiovascular Medicine, Okayama University Graduate School of Medicine Dentistry and Pharmaceutical Sciences, 2-5-1 Shikata-cho, Okayama 700–8558, Japan. Tel.: +81 86 235 7351; fax: +81 86 235 7353.
E-mail address: ichibun@cc.okayama-u.ac.jp (K. Nakamura).

0167-5273/$ – see front matter © 2011 Elsevier Ireland Ltd. All rights reserved.
doi:10.1016/j.ijcard.2011.02.024

Table 1
Clinical data of patients with IPAH.

Patient	Time	Sex	Age	PAP (s/d/m) (mmHg)	mRAP (mmHg)	CI (L/min/m^2)	PVR (dyn/s/cm^5)	BNP (pg/dL)
1	Prior to drug therapy	F	7	150/72/98	4	3.8	1918	136
	Prior to transplantation		13	99/59/72	15	2.3	2779	334
2	Prior to drug therapy	F	28	88/40/59	10	1.9	1416	408
	Prior to transplantation		31	73/30/48	1	2.1	1199	325
3	Prior to drug therapy	F	10	118/67/84	14	2	NA	NA
	Prior to transplantation		13	111/49/67	10	1.7	2438	203
4	Prior to drug therapy	F	NA	NA	NA	NA	NA	NA
	Prior to transplantation		28	113/36/66	7	1.8	3340	50
5	Prior to drug therapy	M	16	163/71/106	2	1.7	2267	14
	Prior to transplantation		20	70/40/50	2	3.3	808	18
6	Prior to drug therapy	F	39	74/23/42	3	2.6	NA	NA
	Prior to transplantation		43	107/47/72	15	2.4	3056	622
7	Prior to drug therapy	F	13	96/50/68	4	2.3	1495	411
	Prior to transplantation		16	83/51/65	8	2.5	784	216
8	Prior to drug therapy	M	NA	NA	NA	NA	NA	NA
	Prior to transplantation		11	130/51/80	9	1.9	2629	420
Mean ± SE	Prior to drug therapy		19 ± 5	mPAP: 76 ± 10	6 ± 2	2.4 ± 0.3	1774 ± 198	242 ± 100
	Prior to transplantation		22 ± 4	mPAP: 65 ± 4	8 ± 2	2.3 ± 0.2	2129 ± 366	273 ± 70

M: male, F: female, PAP: pulmonary artery pressure, s/d/m: systolic/diastolic/mean, mRAP: mean right atrial pressure, CI: cardiac index, PVR: pulmonary vascular resistance, BNP: plasma concentration of brain natriuretic peptide, NA: not available.

is characteristic of a particular cancer cell, rather than non-specifically inhibiting the proliferation of and killing all rapidly dividing cells. Schermuly et al. reported that imatinib reverses pulmonary vascular remodeling and cor pulmonale in rats with monocrotaline-induced PH and in mice with chronic hypoxia-induced PH [8]. Perros et al. reported that PDGF-BB-induced proliferation and migration of PASMCs from patients with IPAH were inhibited by imatinib [10].

Not only inhibition of proliferation but also induction of apoptosis of PASMCs is needed to actively reduce stenosis due to vascular remodeling at small pulmonary arteries of patients with IPAH. These two effects may lead to reverse remodeling of the pulmonary vasculature. Expression of PDGF-B is up-regulated in the medial layer of small pulmonary arteries of rats with monocrotaline-induced PH and imatinib induces apoptosis in the small pulmonary arteries [8]. However, imatinib does not induce apoptosis in cultured IPAH-PASMCs without PDGF treatment [10]. Thus, imatinib may not be able to induce apoptosis in quiescent cells. We hypothesized that imatinib in the presence of PDGF-BB induces apoptosis of PASMCs from patients with IPAH, but that imatinib cannot induce apoptosis in PASMCs without PDGF stimulation. We therefore investigated whether imatinib in the presence and absence of PDGF-BB induces apoptosis of PASMCs from patients with IPAH.

Akt is a member of the serine/threonine-specific kinase family known for facilitating cell survival via the inhibition of apoptotic pathways [12]. Therefore, induction of apoptosis of IPAH-PASMCs may be related to Akt inactivation. We also investigated whether imatinib inhibits Akt activation.

2. Materials and methods

2.1. Isolation, culture and identification of PASMCs

Peripheral segments of the pulmonary artery were obtained at lung transplantation [13] from 8 patients with IPAH as previously described [5,6,14,15] (2 males and 6 females; mean age, 22 ± 4 years; age range 11–43 years) (Table 1). For normal control experiments, samples of pulmonary arteries were also obtained at lung lobectomy from a patient with bronchogenic carcinoma (male, 58 years old) who showed no evidence of PAH and received no systemic chemotherapy or radiation therapy before lung lobectomy as previously described [5,6,14,15]. Samples of the pulmonary arteries were obtained from the most distal area from the carcinoma in the resected lobe. All of the studies were approved by the Ethics Committee of Okayama University Graduate School of Medicine, Density, and Pharmaceutical Sciences, and written informed consent was obtained from all patients before the procedure. The investigation also conforms to the principles outlined in the Declaration of Helsinki.

PASMCs were isolated as described previously [5,6,14–16]. Peripheral segments of pulmonary arteries smaller than 1 mm in outer diameter were disaggregated with collagenase and cut into 2-mm-long sections, and then the adventitia and endothelial cell layers were removed. Vessels were plated on a 6-well plate with Dulbecco's modified Eagle's medium (DMEM; Gibco, Grand Island, NY, USA) supplemented with 10% fetal bovine serum (FBS; Sigma) and 0.1 mg/mL kanamycin (Sigma) and incubated in a humidified 5% CO2 atmosphere at 37 °C. The culture medium was changed every 3 days. After reaching confluence, the cells were subcultured by treatment with trypsin

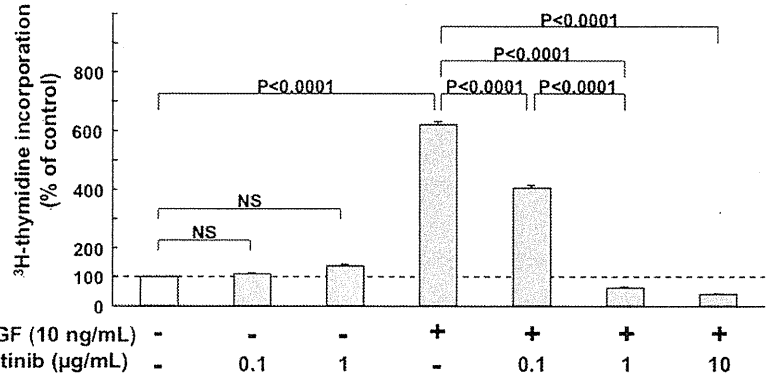

Fig. 1. Inhibitory effect of imatinib on proliferation of PASMCs from IPAH patients. Anti-proliferative effects of imatinib (0.1 to 10 μg/mL) on IPAH-PASMCs stimulated with PDGF-BB (10 ng/mL). ^{3}H-thymidine incorporation was measured. Counts per minute (cpm) were expressed as a percentage of cpm of IPAH-PASMCs treated with a diluent (control). Data are mean ± SE.

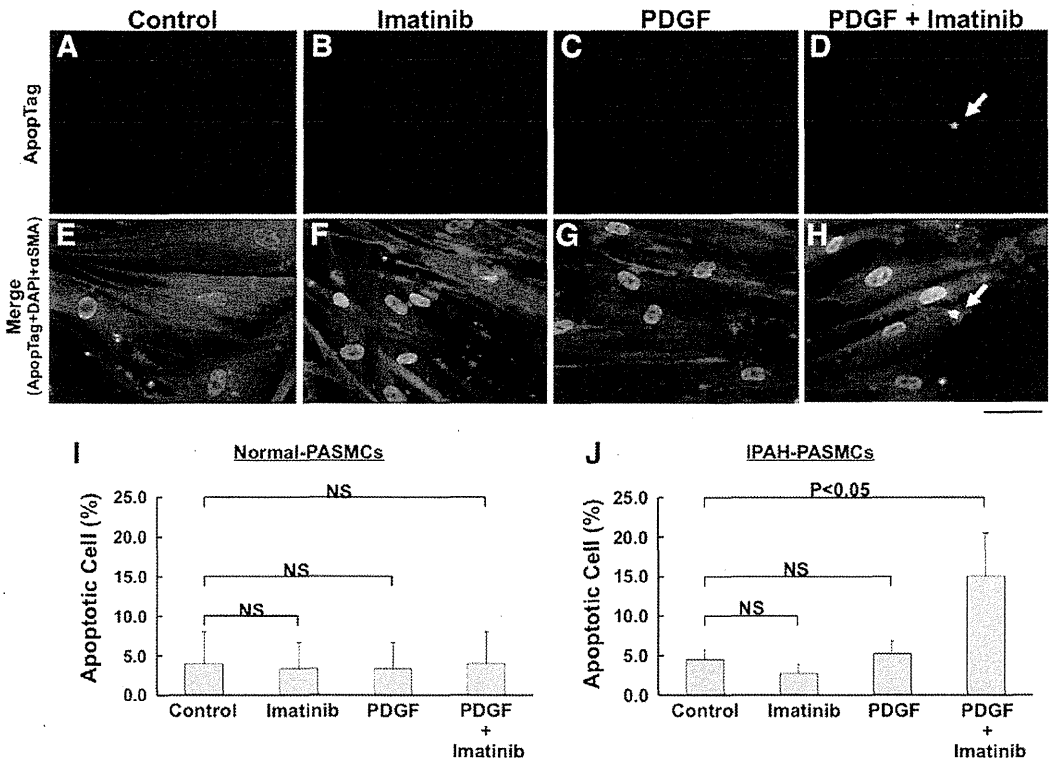

Fig. 2. Effect of imatinib on apoptosis of PASMCs in TUNEL assay by ApopTag fluorescein. A to D, ApopTag fluorescein (green). E to H, Combined images (merge) of ApopTag fluorescein, DAPI (blue) and αSMA (red). A and E, IPAH-PASMCs without treatment. B and F, IPAH-PASMCs treated with imatinib (1 μg/mL). C and G, IPAH-PASMCs treated with PDGF-BB (10 ng/mL). D and H, IPAH-PASMCs treated with imatinib and PDGF-BB. Arrow shows a TUNEL-positive cell (green). Bar = 500 μm. I, Effect of imatinib on apoptosis of normal PASMCs in TUNEL assay. J, Effect of imatinib on apoptosis of IPAH-PASMCs in TUNEL assay. Imatinib (1 μg/mL) in the presence of PDGF-BB (10 ng/mL) significantly increased TUNEL-positive (apoptotic) cells in IPAH-PASMCs compared with the control condition ($P<0.05$). Data are mean ± SE.

(0.05%)/ethylenediaminetetraacetic acid (EDTA) (0.02%). Cell identification was confirmed by the examination of cytoskeletal components (α-smooth muscle actin, myosin, and smoothelin) using an immunocytochemical technique as described previously [5,15]. Cells between passages 3 to 5 were used for all experiments.

2.2. Effects of imatinib on cell proliferation

To assess the antiproliferative effect of imatinib on PASMCs, we measured ^{3}H-thymidine incorporation using methods described previously [5,16]. PASMCs were reseeded in 24-well plates at a density of 5×10^4cells/well on day 0. After 16 h of incubation (on day 1), the culture media were replaced with low-serum culture media (DMEM, 0.1% FBS, and 0.1 mg/mL kanamycin), and the cultured cells were made quiescent for 48 h. On day 3, PDGF-BB (10 ng/mL) (Sigma), imatinib (0.1 to 10 μg/mL) (Novartis) or an Akt inhibitor, Akt-I-1/2 (1 μmol/L) (Calbiochem), was added to the media. After 21 h (on day 4), the cells were labeled with ^{3}H-thymidine at 1 μCi/mL for 3 h. After completion of labeling, the cells were washed with ice-cold PBS, fixed with 5% trichloroacetic acid and 95% ethanol, and lysed with 200 μL/well of 0.33 mol/L NaOH. Aliquots of the cell lysates were neutralized with 1 mol/L HCl, and the radioactivity was measured in a liquid scintillation analyzer (TRI-CARB 2200CA; Packard, Downers Grove, IL, USA).

2.3. Western blot analysis

PASMCs from patients with IPAH were prepared in the same manner as that described for analysis of DNA synthesis. They were treated in the presence or absence of PDGF-BB (10 or 100 ng/mL), imatinib (1 or 10 μg/mL) and a mitogen-activated protein kinase/extracellular signal-regulated kinase (MEK) inhibitor, U0126 (3 μmol/L) (Promega). Western blot analysis was performed as described previously [5,7]. Briefly, total cell lysates of cultured PASMCs were extracted in commonly used radioimmunoprecipitation (RIPA) buffer with 10 mg/mL phenylmethylsulfonyl fluoride (Sigma) and then concentrated by centrifugation at 12,000 rpm for 20 min. Protein samples (10 μg) were loaded on 10% sodium dodecyl sulfate-polyacrylamide gel and blotted onto nitrocellulose membranes. Blots were incubated with rabbit anti-p27 antibody (Santa Cruz Biotechnology), anti-GAPDH antibody (Chemicon), anti-phospho-Akt antibody and anti-total-Akt antibody (Cell Signaling Technology Inc., Beverly, MA). The relative integrated density of each protein band was digitized by NIH image J 1.34 s.

2.4. Evaluation of apoptosis

TUNEL assays were performed using an ApopTag fluorescein in situ apoptosis detection kit (Chemicon International Inc.) according to the manufacturer's instructions as described previously [17]. Nuclear morphology was examined by labeling with DAPI solution (0.6 μg/mL, Dojindo Laboratories). Immunofluorescence staining was performed to confirm α-smooth muscle actin (αSMA) expression using αSMA antibody (1:100 dilution, Sigma). Caspase assay was performed using a CaspaTag Caspase-3/7 in situ apoptosis detection kit (Chemicon International Inc.) according to the manufacturer's instructions. Nuclear morphology was examined by Hoechst staining. The samples were analyzed by fluorescence microscopy (Olympus IX71, Olympus Optical Co. Ltd, Tokyo, Japan). For each cover slip, 5–10 fields (with 10–30 cells in each field) were randomly selected to determine the percentage of apoptotic cells in total cells based on the morphological characteristics of apoptosis. PASMCs were reseeded on collagen-coated glass cover slips in 12-well plates at a density of 5×10^4 cells/well on day 0. After 16 h of incubation (on day 1), the culture media were replaced with low-serum culture media (DMEM, 0.1% FBS, and 0.1 mg/mL kanamycin), and the cultured cells were made quiescent for 48 h. On day 3, PDGF-BB (10 ng/mL), imatinib (1 μg/mL) or Akt-I-1/2 (1 μmol/L) was added to the media. After 24 h (on day 4), the cells were stained by using an ApopTag fluorescein in situ apoptosis detection kit or CaspaTag in situ apoptosis detection kit.

Transmission electron microscopy was performed with an electron microscope (H-7100: Hitachi; Tokyo, Japan).

To observe cellular apoptosis with a time-lapse system (Olympus Optical Co.), PASMCs were cultured on a 35-mm culture dish that has a micro-photolithographed squared pattern (Kuraray Co., Ltd., Tsukuba, Japan) [7] so that the apoptotic cells will not disappear from view.

2.5. Statistical analysis

All results are expressed as mean ± SE. Statistical significance for comparison between the two measurements was determined using Student's *t* test. For comparison between the different treatment groups, statistical analysis was performed using one-